ARCTIC SEA ICE: SATELLITE OBSERVATIONS, GLOBAL CLIMATE MODEL PERFORMANCE, AND FUTURE SCENARIOS

By

Tracy S. Rogers

Recommended:

Advisory Committee Chair

Department Chair, Resources Management

Approved:

Dean, School of Natural Resources & Agricultural Sciences

Dean of the Graduate School

Aug 1, 2011

Date

ARCTIC SEA ICE: SATELLITE OBSERVATIONS, GLOBAL CLIMATE MODEL PERFORMANCE, AND FUTURE SCENARIOS

A

THESIS

Presented to the Faculty

of the University of Alaska Fairbanks

in Partial Fulfillment of the Requirements

for the Degree of

MASTER OF SCIENCE

BY

Tracy S. Rogers, B.A.

Fairbanks, Alaska

August 2011

Abstract

This thesis examined Arctic sea ice trends through observational records and model-derived scenarios. A regional analysis of Arctic sea ice observations 1980-2008 identified regional trends similar to the pan-Arctic. However, winter maximum (March) extent in the Atlantic quadrant declined faster. Through an analysis of Atlantic Ocean temperatures and Arctic winds, we concluded that melting sea ice extent may result in increased Atlantic Ocean temperatures, which feeds back to further reductions in Atlantic quadrant extent. Further, Arctic winds do not appear to drive Atlantic ice extent. We evaluated performance of 13 Global Climate Models, reviewing retrospective (1980-2008) sea ice simulations and used three metrics to compare with the observational record. We examined and ranked models at the pan-Arctic domain and regional quadrants, synthesizing model performance across several Arctic studies. The top performing models were able to better capture pan-Arctic trends and regional variability. Using the best performing models, we analyzed future sea ice projections across key access routes in the Arctic and found likely reduced ice coverage through 2100, allowing increasingly longer marine operations. This unique assessment found the Northwest and Northeast Passages to hold potential for future marine access to the Arctic, including shipping and resource development opportunities.

Table of Contents

Page

List of Tables

List of Figures

Acknowledgements

I'd like to thank John Walsh, Scott Rupp, Lawson Brigham, and Mike Sfraga for being my graduate advisory committee. All four committee members were important in the design and review of this study. In addition, John Walsh oversaw the more technical aspects of the first two chapters. Scott Rupp served as my primary advisor, and spent many hours editing this thesis into its present form. Lawson Brigham was the key advisor in designing and reviewing the third chapter. Mike Sfraga helped initiate this thesis by introducing me to the rest of my committee. Thanks to William Chapman for his help in retrieving the National Snow and Ice Data Center sea ice data and for providing the National Centers for Environmental Prediction and National Center for Atmospheric Research reanalysis ocean sea surface temperature dataset. Thanks to Tom Kurkowski and Dustin Rice for helping with IT related support. Thanks also to Steve Seefeldt and Sherry Modrow for their thoughtful reviews. This work was supported by the University of Alaska, Fairbanks' International Arctic Research Center through the National Science Foundation's Office of Polar Programs and by the Scenarios Network for Alaska and Arctic Planning. All statistical analyses were performed using the R language and environment for statistical computing and graphics. For more information, see http://www.r-project.org/.

Introduction

The circumpolar Arctic region has experienced significant, complex climatic changes on land, in the oceans, and in the atmosphere. The Arctic's amplification of climate change combined with its sensitivity to even minor modifications in forcing has resulted in significant changes to both terrestrial and marine ecosystems and related human livelihoods. Declining sea ice is a key indicator of Arctic vulnerability to the effects of climate change (ACIA, 2005).

Records of early sea ice observations date to the 18th and 19th centuries, as explorers sought marine routes north of Canada and Russia. More complete observations of sea ice began in the 1930s, with the advent of air traffic over Arctic regions, and expanded during the post-World War II era, when nuclear submarine sonar data began to cover large areas of the Arctic (AMSA, 2009). Most recently (1979-present), scientists have tracked sea ice changes using passive microwave satellite observations, which allow for in-depth analyses of sea ice trends (Cavalieri et al., 1996; Meier et al., 2006).

Since 1979, Arctic sea ice extent (SIE) in September has declined by more than 30 percent (Parkinson and Cavalieri, 2008). Further, little multi-year sea ice remains in the Arctic, which indicates that volume has also significantly declined since 1979 (Perovich et al., 2010). These changes are expected to continue, with the likelihood of larger and faster changes in the future (ACIA, 2005; IPCC, 2007). Snow covered sea ice reflects as much as 90 percent of the Sun's energy, whereas open water reflects as little as 10 percent of incoming solar radiation. As sea ice retreats, the amount of energy the Earth absorbs from the Sun increases significantly, leading to faster decline of SIE and increased warming (ACIA, 2005).

Satellite observations of sea ice reveal a dramatic decrease in SIE between 2001 and 2010 (Stroeve et al., 2011), and eight of the ten lowest September SIEs have occurred since 2001 (Fetterer et al., 2009; Richter-Menge and Overland, 2010). Further, using sediment cores as a proxy, a comparison of sea ice conditions over the past 2,000 years to current conditions revealed that 2001-2010 has the least ice coverage and the quickest decline in SIE (Polyak et al., 2010). Recent changes in the Arctic suggest that

understanding sea ice loss is critical to our understanding of Arctic changes and feedbacks to the global climate system (ACIA, 2005).

This research seeks to better understand changing sea ice in the Arctic. Specifically, this study builds upon and expands previous research on Arctic sea ice and modeling. Chapter 1 investigates regional variations in observed SIE. Previous studies that have investigated regional sea ice trends evaluated the Arctic using divisions based on the geographic location of seas. In contrast, we use the longitudinal regions defined in the ACIA, which was designed for understanding the human impacts of climate change – seeking to improve knowledge about sea ice changes as well as providing new information for understanding human dimensions. Describing changes in sea ice within the same regions offers additional ways to assess physical, social, and economic impacts. Evaluating regional changes in SIE contributes to our understanding of climate impacts, especially important because sea ice plays such an important role in Arctic habitats (ACIA, 2005). Understanding sea ice loss in different regions can also help to improve regional output of Atmosphere-Ocean General Circulation Models (AOGCMs) (Overland and Wang, 2007).

Development of AOGCMs began in the mid-1970s, but models were rudimentary and focused only on the atmosphere. By the Second Assessment Report of the IPCC in 1995, AOGCMs were used to model climate changes and included land surface, ocean, and sea ice. In the IPCC Third Assessment Report in 2001, AOGCMs advanced significantly, including more coupled models, many of which included ice dynamics. The 2007 IPCC AR4 report included sea ice as an output of nearly all AOGCMs (IPCC, 2007). In a simplified sense, sea ice models use atmospheric and oceanic temperature and circulation to determine freeze and thaw patterns. As scientific understanding of sea ice and climate models has progressed, climate modelers have been able to more reliably reproduce sea ice melt and thaw patterns from 1900-2000 (IPCC, 2007).

Model projections suggest the climate system may warm more than twice as much during this century as it did in the past century, which will result in widespread reductions in snow and ice cover and increases in sea level (IPCC, 2007). A majority of

climate models used in the AR4 suggest the complete or near-complete loss of summer sea ice between 2060 and 2100 (IPCC, 2007). While most climate model projections do not predict an ice-free Arctic summer until closer to the end of this century, these models have several limitations, including underestimation of recent trends of sea ice (Stroeve et al., 2007). Through the use of climate models and current sea ice trends, some studies have concluded that a seasonally sea ice-free Arctic is possible sooner than 2050 (Stroeve et al., 2007; Comiso et al., 2008; Maslowski et al., 2008; Wang and Overland, 2009; Zhang, 2010). The current range of future sea ice scenarios emphasizes the importance of understanding the limitations of AOGCMs and illustrates the significance of accurately portraying sea ice dynamics

Chapter 2 evaluates AOGCM performance in terms of SIE comparing observations in the Arctic with retrospective simulations using the same regions as in the first chapter. Evaluating current model performance is a good first step in understanding changes in sea ice. By analyzing the performance of these models, we can better understand which approaches to sea ice modeling hold the most potential and we can use those models to investigate future sea ice scenarios. Overland and Wang (2007) have also reviewed regional model performance, evaluating GCMs in regional Arctic seas. Their study and the present study differ in the evaluation regions used.

Decreasing SIE has signaled the need for understanding possible future changes. Chapter 3 applies the best performing models identified in Chapter 2 to investigate future projections of sea ice. Using these projections, we discuss future Arctic marine shipping routes.

Observational records show that changes are occurring faster with each decade, such that even the most extreme sea ice simulations from AR4 are not keeping pace (IPCC, 2007; Stroeve et al., 2011). Over the past decade (2000-2010), sea ice conditions have allowed greater access to the Arctic Ocean by marine transport. The Arctic Marine Shipping Assessment (AMSA, 2009) examined Arctic sea ice observations and model simulations, reviewing social, economic, environmental, and political implications of increasing Arctic marine navigation. AMSA used projections from the Hadley Centre

GEM1 for March and September of 2010-2030, 2040-2060, and 2070-2090. These projections indicated decreasing sea ice conditions in the future, with the possibility of a sea ice-free summer by the end of the century (AMSA, 2009). However, several studies have used AOGCM projections to estimate future sea ice conditions, and found this estimate conservative (Stroeve et al., 2007; Wang and Overland, 2009; Zhang, 2010; Stroeve et al., 2011).

Zhang (2010) analyzed the performance of models from 1979-2004. Using the eight models that performed best, Zhang concluded the Arctic is likely to see an ice-free summer – defined as having less than one-million square kilometers of sea ice – between 2037 and 2065. Wang and Overland (2009) conducted an analysis of model performance, and came to the conclusion that ice-free conditions could come as soon as 2040. Boé et al. (2009) projected that summer sea-ice cover would vanish before 2100. Stroeve et al. (2007) concluded the Arctic would see a sea ice-free summer between 2050 and 2100, but also recognized that models significantly underestimated sea ice decline and sea ice could disappear even sooner than 2050.

While the AMSA study investigated the possibility of future marine routes using Hadley Centre GEM1 projections, no previous studies have extensively reviewed the currently available models, and then used the best performing models to provide a suite of projections for future Arctic marine access, making this chapter unique in its breadth and scope.

CHAPTER 1

REGIONAL VARIATIONS IN ARCTIC SEA ICE EXTENT AND THE ROLE OF WINDS AND OCEAN TEMPERATURES[1]

1.1 Abstract

The widely cited loss of pan-Arctic sea ice is not similar in all regions of the Arctic. Further, the relative importance of wind and sea surface temperatures as drivers of sea ice patterns can be expected to vary regionally. While ice extent in three quadrants has followed trends similar to pan-Arctic patterns, sea ice in the Atlantic quadrant decreased much faster in March than the pan-Arctic trend. We tested our hypothesis that warmer Atlantic waters are quickening the rate of decline in the Atlantic quadrant's March sea ice extent, whereas Arctic summer winds move sea ice from other quadrants into the Atlantic quadrant, masking September sea ice loss. Results indicate that Atlantic sea ice loss may instead be leading to warmer Atlantic Ocean sea surface temperatures, while trans-polar winds do not appear to drive Atlantic sea ice extent. The results of this research suggest that sea ice may be a primary driver in warming sea surface temperatures, but was unable to identify a driver to explain the loss of winter or summer Atlantic quadrant sea ice.

[1] Rogers, T., Walsh, R., and Rupp, T.S. Regional Variations in Arctic Sea Ice Extent and the Role of Winds and Ocean Temperatures. Prepared for submission to *Arctic*.

1.2 Background

From 1980 through 2008, minimum (September) pan-Arctic SIE decreased by 10.7 percent per decade and maximum (March) pan-Arctic SIE decreased by 2.8 percent per decade. However, the widely cited loss of pan-Arctic sea ice is not similar in all regions of the Arctic. Previous Arctic sea ice studies developed sub-regions, investigating seas that were ice-covered or partially ice-covered for some or all of the year. The most recent of these studies measured a significant decline in SIE year round, with the largest declines in the summer. These results differed from earlier studies in that winter sea ice losses had not reached significance (Meier et al., 2007; Parkinson and Cavalieri, 2008). A particular interest of this study is the Atlantic sector, where our preliminary analysis indicated that SIE is decreasing as rapidly in winter as in summer, and much more rapidly in winter than the other regions, a trend not identified in previous studies.

Previous research has noted that rising ocean temperatures in the Pacific and Atlantic Oceans are quickening the decline of sea ice and slowing winter freeze-up. Pacific and Atlantic Ocean temperatures have been increasing over the past 30 years, which has in turn brought warmer water further into the Arctic Ocean, reducing SIE (Francis and Hunter, 2007; Shimada et al., 2006). The warming Atlantic Ocean could explain the rapid decrease in winter SIE over the past 30 years in the Atlantic region. Studies have also shown correlations between winds and sea ice movement in the Arctic. During summer months pan-Arctic winds move sea ice towards the Fram Strait, increasing the rate of decreasing sea ice cover in the Arctic (Ogi et al., 2008; Ogi et al., 2010). However, this could potentially increase the quantity of sea ice in the Atlantic quadrant during summer months.

The objectives of the present study are to investigate the differences in SIE loss by geographical sector and examine potential drivers. Specifically, we test the hypothesis that warmer Atlantic waters are quickening the rate of decline in the Atlantic quadrant winter SIE, whereas Arctic summer winds move sea ice from other quadrants into the Atlantic quadrant, masking summer sea ice loss.

1.3 Data and Methods

Observed SIE data from 1980 to 2008 were obtained from the National Snow and Ice Data Center's (NSIDC) passive microwave data set (Cavalieri et al., 1996; Meier et al., 2006). These data are comprised of four sets of satellite data: Nimbus-7 SMMR (January 1980 - August 1987), DMSP-F8 SSM/I (July 1987 - December 1991), DMSP-F11 SSM/I (December 1991 – September 1995), and DMSP-F13 SSM/I (May 1995 – December 2008). Sea ice concentrations come from a revised NASA Team algorithm (Cavalieri et al., 1996).

The sea ice data were interpolated from the original 25km resolution to one degree latitude by one degree longitude for the purpose of simplifying the calculation of monthly SIE. A comparison between pixel resolutions indicates our estimated September data underestimates SIE by five to seven percent, while demonstrating the same inter-annual variability and trend slope as NSIDC's SIE archive (Fig. 1.1). The difference in estimated and archived SIE is due to land-sea mass classification that changes with a coarser grid resolution. In our conversion methodology, more coastal regions were converted into land than sea, reducing coastline SIE. Each pixel with sea ice presence (15 percent or more sea ice) was converted into a square kilometer estimate using 12 347 km^2 (area inside a one latitude by one longitude pixel at the equator) multiplied by the cosine of the latitude. Areas with ice present were summed to estimate the total SIE in each region.

The Arctic was divided into four quadrants: 46° W to 45° E (Atlantic quadrant), 46° E to 135° E (Russian quadrant), 136° E to 135° W (Pacific quadrant), and 136° W to 45° W (Canadian quadrant) and was based on the divisions used by the ACIA (Fig. 1.2; ACIA, 2005). We conducted a time-series analysis of SIE trends across the Arctic and in each quadrant. We performed linear regression analysis and used a least squares fit approach and an f-test for confidence intervals.

National Centers for Environmental Prediction (NCEP) and National Center for Atmospheric Science (NCAR) reanalysis data were used for Atlantic Ocean temperature values: the average sea surface temperatures (SSTs) in degrees Celsius from 75° N to 80°

N, and 20° W to 70° E (Kalnay et al., 1996). NCEP/NCAR reanalysis data were also used for wind magnitudes in the Arctic (Kalnay et al., 1996). We used eight equally spaced points from 72° N to 90° N along the 180 meridian at the surface to estimate Arctic wind magnitudes. Since these winds are meridional, a positive value represents southerly winds, whereas a negative value represents northerly winds. We tested several sets of grouped months, which we call multi-month periods: January-September, February-May, April-July, April-September, June-July, June-August, and October-September. We used linear regression analysis to evaluate the relationship between the variables and the strength of that relationship.

We investigated Atlantic Ocean SSTs to explain the anomalous winter Atlantic SIE. The regression analysis of March and September SIE used Atlantic Ocean SSTs from the 12 months prior. For example, March SIE is regressed with the average temperature from March of the previous year to February of the present year. This was done to investigate the effect that SSTs have on SIE in the months of either March or September, rather than using the standard January-December average for a year. The average values computed for March through February are shown in Figure 1.3.

For the Atlantic quadrant, September SIE was tested against wind magnitudes in the Arctic Ocean along the Dateline averaged over several multi-month periods. Figure 1.4 shows average wind magnitudes in June-July for 1980 through 2008. We used points along the 180° meridian because those are in line with the trans-polar drift. To validate our wind tests, we compared our results to previous research on wind fields and pan-Arctic SIE, namely that of Ogi et al. (2010). Specifically, Ogi et al. found that 50 percent of the variation in September SIE comes from winter and summer wind forcing. We used a streamlined sampling of winds as a substitute for the trans-polar drift, yet found similar results to Ogi's work. Against pan-Arctic SIE, five of the seven multi-month periods tested reached significance, and April-September winds accounted for 51 percent of the variation in September SIE (Table 1.1). These tests confirm the importance of the transpolar drift to Arctic SIE, found in previous research (Ogi et al., 2010).

1.4 Results

Pan-Arctic minimum SIE (September) decreased at a rapid rate from 1980-2008, while maximum SIE (March) declined at a slower rate (Table 1.2). A regional evaluation of sea ice trends identified significant variation between regions (Table 1.3). The Russian and Pacific quadrants had similar or greater declines in September SIE than the pan-Arctic and Russian quadrant, while the Canadian and Atlantic quadrants' losses were less rapid (Fig. 1.5). In March, SIE loss in the Canadian, Pacific, and Russian quadrants and the pan-Arctic was much slower than Atlantic quadrant SIE loss (Fig. 1.6).

All quadrants and the pan-Arctic revealed significant relationships for time series of September and March SIE (1980 to 2008). Pan-Arctic, September SIE loss was 10.7 percent per decade, while individual quadrants losses were between 6.7 and 15 percent per decade. Pan-Arctic, March SIE loss was 2.8 percent per decade, three quadrants losses were between 1.4 and 2.7 percent, while the Atlantic quadrant loss was 7.8 percent per decade (Table 1.2; Table 1.3).

Some interesting trends emerge in our breakdown of SIE trends. In our pan-Arctic analysis, the greatest SIE loss was in September, where the trend exceeded ten percent per decade, and the least SIE loss occurred in February and March, where SIE loss was less than three percent per decade. July and August SIE losses were also well ahead of other months, -6.6 and -8.7 percent per decade, respectively. The Russian, Pacific, and Canadian quadrants all had similar results, although the Canadian quadrant had its greatest SIE loss in July, whereas the Russian quadrant had its greatest loss in August. In all three of these quadrants, months with SIE loss exceeding seven percent occurred between July and November. In the Atlantic quadrant, November through April all had SIE losses greater than seven percent per decade, whereas all months between May and October decreased by less than seven percent. Further, because SIE loss in winter months was much greater in the Atlantic quadrant than in the pan-Arctic, the Atlantic quadrant lost annual SIE at almost double the pan-Arctic rate (Table 1.2; Table 1.3). A disproportionate loss of pan-Arctic sea ice in March occurs in the Atlantic quadrant (Fig. 1.7). A signal to noise ratio indicates that the time series are significantly more signal

than noise (Table 1.4). As expected, the quadrants with greater SIE losses in the summer also had larger signal to noise ratios in the summer than in winter; the Atlantic quadrant had larger ratios in the winter than in summer. However, pan-Arctic signal to noise ratios were similar throughout the year.

A linear regression of Atlantic quadrant, March SIE and average SSTs had a statistical significance at the 99.9 percent level (R^2=0.51). An identical regression using the Russian quadrant also had a 99.9% significance level (R^2=0.39), but neither the Pacific nor Canadian quadrants reached significance at even 95 percent level (Table 1.5). This indicates the SSTs were correlated with the decrease in SIE in the Atlantic quadrant. To further investigate the role that SSTs may be having on pan-Arctic and Atlantic quadrant SIE, we investigated one year lagged regressions on the data and examined de-trended data (Table 1.6). The de-trended Atlantic SIE resulted in increased significance when the SIE leads SSTs as compared to the non-lagged regression. However, if the SSTs lead SIE, the regression loses significance. These results show that Atlantic region SIE both has a correlation with and precedes changes in North Atlantic SSTs. However, the results do not exclude the possibility that a common driver is responsible for changes in both variables – the third requirement of causality.

When tested against Atlantic SIE in September, June-July wind magnitude is the only period that reached significance at the 95 percent level (R^2 = 0.12). The other multi-month periods that were tested did not correlate with Atlantic quadrant SIE, which suggests that Arctic wind magnitudes do not have an important relationship with September Atlantic SIE. However, when tested against Pacific SIE, Arctic wind magnitudes through almost all multi-month periods reached significance with September SIE (Table 1.7). Since Arctic wind magnitudes had a negative correlation with Pacific sea ice, it follows that Arctic winds are pushing Pacific-sector ice into the other three quadrants, but that the signal is not being seen in the Atlantic quadrant.

Linear regressions confirm correlations between September Atlantic SIE and Atlantic Ocean SSTs (Table 1.5). An analysis was conducted to determine if Arctic wind patterns would have a higher correlation with Atlantic SIE if coupled in a regression with

SSTs. The significance that wind has on Atlantic quadrant SIE improved for most of the multi-month periods, but only two multi-month periods reached statistical significance: June-July and June-August. The other multi-month periods did not reach a 95 percent significance level (Table 1.8). These results again suggest an absence of correlation between the Atlantic quadrant SIE and Arctic winds.

The multiple linear regressions for SSTs and wind magnitudes were repeated for SIE in the other three quadrants. Russian quadrant SIE reached significance for April-September and June-August for wind magnitudes, and for no multi-month periods when using the coupled regression. The Pacific quadrant SIE reached significance for all multi-month periods for wind magnitudes except June-July, and all multi-month periods once combined with SSTs. The Canadian quadrant reached significance for January-September, April-September, June-July, and October-September with wind magnitudes. When coupled with SSTs, the Canadian quadrant reached significance for January-September, April-September, and June-July. These results show that different time periods of winds have differing correlations with each quadrant. April-September winds had a significant effect in three of the four quadrants and the pan-Arctic, which suggests that time period is important for ice movement in the Arctic.

1.5 Conclusions and Discussion

Reductions in SIE will have broad effects on regional climate systems, marine ecosystems, and the people who live throughout the circumpolar Arctic. Given the reliance of Arctic Indigenous peoples on sea ice, it is important to understand how sea ice is changing within regions. People need to have tools for developing future scenarios of regional impacts and understanding regional changes in sea ice is a crucial factor. Better understanding of the mechanisms behind these changes allows for improved modeling techniques and greater accuracy for future scenarios (IPCC, 2007; ACIA, 2005). Our investigation examined how ocean temperatures and wind magnitudes are connected to observed variations in regional SIE.

Our investigation of the passive microwave satellite record (1980-2008) identified important regional variations in observed Arctic SIE. All quadrants of the Arctic exhibited statistically significant, declining sea ice trends. However, in the Atlantic quadrant, March SIE is declining at a much faster rate than in the other quadrants, a trend that has not been noted in previous studies. In the Atlantic quadrant, SIE decreased at a faster rate (in percent/decade) for all months from November through April than for any months from May through October (Table 1.3). In the pan-Arctic and other quadrants, the months with the most rapid decline of SIE ranged from late summer through early fall.

The first part of our hypothesis was that warming Atlantic Ocean SSTs were resulting in decreased winter SIE in the Atlantic quadrant. The results of our analyses indicated SSTs are correlated with September SIE trends in all quadrants of the Arctic and also for March SIE trends in both the Atlantic and Russian quadrants. However, in contrast to our hypothesis, SIE in the Atlantic may result in warmer SSTs. This indicates that some stronger influence, likely air temperatures or Pacific SSTs, is resulting in reduced SIE in the Atlantic. Reduced SIE would then have a lesser cooling effect on northern Atlantic SSTs, resulting in warming.

The second part of our hypothesis was that Arctic winds were moving sea ice from the Pacific quadrant, into the Atlantic quadrant, increasing summer SIE. Our analyses suggest that wind magnitude associations do not appear to be increasing the quantity of sea ice in the Atlantic quadrant – the most statistically significant relationships between sea ice and Arctic winds were for the Pacific quadrant and the pan-Arctic domain. Finally, the combined influence of Arctic wind magnitudes and SSTs showed little impact on the Atlantic quadrant, but some on the Pacific quadrant sea ice (Table 1.5; Table 1.6; Table 1.7). Our results suggest wind magnitudes have a strong effect on diminishing SIE in the Pacific quadrant and pan-Arctic SIE, which supports previous studies (Table 1.1; Ogi et al., 2010).

Understanding regional variations in SIE may be requisite for accurate model projections of future sea ice dynamics. Improving sea ice models will be of critical importance in providing the information required to develop sound management

strategies and informed policy. Further, this translates into a greater scientific understanding of changing ecosystems, empowering individuals, communities, and societies to adapt to impacts of climate change.

1.6 Tables

Table 1.1 Pan-Arctic SIE and wind magnitude. The results of linear regression analysis between pan-Arctic SIE and wind magnitudes. Standard typeface represents 95 percent significance; italics represent significance of 99 percent; bold represents significance of 99.9 percent or greater; and NS represents no significance at 95 percent.

Multi-Month Period	**R^2**
January-September	**0.328**
February-May	NS
April-July	*0.2785*
April-September	**0.51**
June-July	NS
June-August	*0.251*
October-September	*0.243*

Table 1.2 Pan-Arctic SIE, 1980-2008. Average values from 1980-2008, the standard deviation for that period, the trend, and the decadal trend are given for each month. For the trend percent per decade, the annual trend and all months reached significance at 99.9 percent or greater.

	Average, 1980-2008	**Std Dev. 1980-2008**	**Trend**	**Trend**
Time	10^6 km^2	10^6 km^2	10^3 km^{2}a^{-1}	% decade^{-1}
Annual	11.5	0.50	-53.8	-4.3
Jan.	14.2	0.49	-49.8	-3.2
Feb.	15.0	0.47	-47.1	-2.9
Mar.	15.2	0.48	-46.4	-2.8
Apr.	14.3	0.47	-46.4	-3.0
May	13.0	0.44	-37.5	-2.7
June	11.4	0.42	-42.8	-3.4
July	9.3	0.70	-70.9	-6.6
Aug.	6.9	0.74	-71.7	-8.7
Sept.	6.3	0.86	-82.2	-10.7
Oct.	8.5	0.60	-53.4	-5.6
Nov.	10.6	0.56	-55.4	-4.7
Dec.	12.6	0.45	-41.6	-3.0

Table 1.3 Regional SIE loss per decade. Trend percent per decade calculated for each month for the four quadrants, and annual trend percent per decade. Standard typeface represents 95 percent significance; italics represent significance of 99 percent; bold represents significance of 99.9 percent or greater; and underline represents no significance at 95 percent.

Time	Atlantic	Russian	Pacific	Canadian
Annual	**-7.6**	**-3.7**	**-3.2**	**-4.4**
Jan.	**-9.4**	**-2.7**	-0.8	*-3.4*
Feb.	**-8.5**	*-2.2*	-1.0	*-2.8*
Mar.	**-7.8**	-1.4	-1.6	-2.7
Apr.	**-8.0**	-1.7	-2.1	-2.4
May	**-6.8**	-2.4	-1.3	**-2.5**
June	**-5**	*-3.8*	-1.2	**-4.7**
July	*-6.1*	**-8.1**	*-2.4*	**-10.1**
Aug.	-6.8	**-10.0**	**-9.6**	**-7.3**
Sept.	-6.7	*-9.5*	**-15.0**	**-6.2**
Oct.	-5.6	-3.1	**-6.5**	**-6.3**
Nov.	**-7.1**	-2.4	*-2.7*	**-7.3**
Dec.	**-9.4**	**-2.5**	-0.7	*-2.9*

Table 1.4 Arctic SIE time series' signal to noise ratio. These ratios represent the strength of the trend within the dataset, also known as a signal to noise ratio. This is calculated by taking the difference between the fitted values for 1980 and 2008, and dividing that by the standard deviation. A value of one or greater indicates that the trend is more dominant than the noise.

Time	Pan-Arctic	Atlantic	Russian	Pacific	Canadian
Annual	3.0	2.5	2.1	2.2	2.5
January	2.8	2.2	2.1	0.6	1.8
February	2.8	2.2	1.8	0.9	1.8
March	2.7	2.3	1.4	1.3	1.5
April	2.7	2.4	1.3	1.3	1.5
May	2.4	2.1	1.4	0.7	2.0
June	2.9	2.0	1.8	1.2	2.5
July	2.8	1.7	2.3	1.6	2.5
August	2.7	1.4	2.0	2.1	2.2
September	2.7	1.4	1.6	2.5	2.1
October	2.5	1.5	0.9	2.0	1.9
November	2.8	2.1	1.4	1.9	2.2
December	2.6	2.2	1.9	0.5	1.7

Table 1.5 Atlantic Ocean SSTs and Arctic SIE. The results of linear regressions between SSTs and SIE loss in September and March by region. Italics represent significance of 99 percent; bold represents significance of 99.9 percent or greater; and NS represents no significance at 95 percent.

Quadrant	September R^2	March R^2
Pan-Arctic	**0.49**	**0.47**
Atlantic	*0.21*	**0.51**
Russian	**0.48**	**0.39**
Pacific	*0.26*	NS
Canadian	*0.13*	NS

Table 1.6 Lag correlations: Atlantic Ocean SSTs and Arctic SIE. The results for one year lag regressions between SIE and SSTs. The bottom half shows the results after the trend for the time series of SIE and SSTs have been removed. Standard typeface represents 95 percent significance; italics represent significance of 99 percent; bold represents significance of 99.9 percent or greater; and NS represents no significance at 95 percent.

	No Lead	**SIE Leads**	**SSTs Lead**
Pan-Arctic	**0.47**	**0.62**	*0.26*
Atlantic	**0.5**	**0.68**	0.17
De-trended			
Pan-Arctic	NS	NS	NS
Atlantic	0.15	**0.43**	NS

Table 1.7 Pacific SIE and Pacific wind magnitude. The results for Pacific wind magnitudes on Pacific quadrant SIE in September. Standard typeface represents 95 percent significance; italics represent significance of 99 percent; bold represents significance of 99.9 percent or greater; and NS represents no significance at 95 percent.

Month Period	**R^2**
January-September	**0.52**
February-May	*0.19*
April-July	**0.34**
April-September	**0.58**
June-July	NS
June-August	*0.28*
October-September	**0.44**

Table 1.8 Atlantic SIE, Arctic wind magnitude, and Atlantic Ocean SSTs. The results of a multiple linear regression of Arctic wind magnitudes and Atlantic Ocean SSTs on September SIE in the Atlantic quadrant. Sig(O) represents the statistical significance that average annual ocean temperatures had on September SIE, and Sig(W) represents the statistical significance that the given month period's wind magnitudes had on SIE. The r-squared represents the combined r-squared from these two values.

Month Period	R^2	Sig(O)	Sig(W)
January-September	0.28	99%	NS
February-May	.18	99%	NS
April-July	.18	99%	NS
April-September	.24	99%	NS
June-July	0.37	99%	99%
June-August	0.34	99.9%	95%
October-September	0.28	99%	NS

1.7 Figures

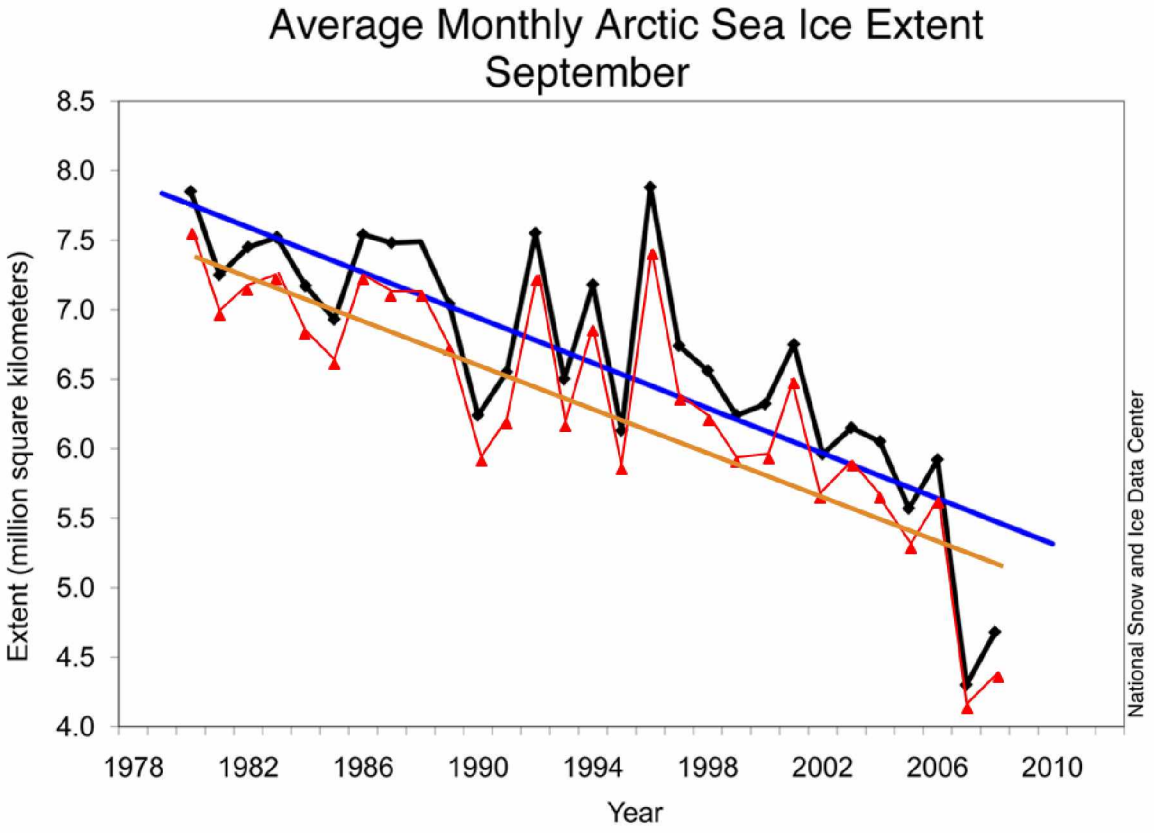

Figure 1.1 Average monthly Arctic SIE, 1980-2008. A comparison of SIE between the official NSIDC calculations, in black with a blue trend line, and our calculations, in red with an orange trend line.

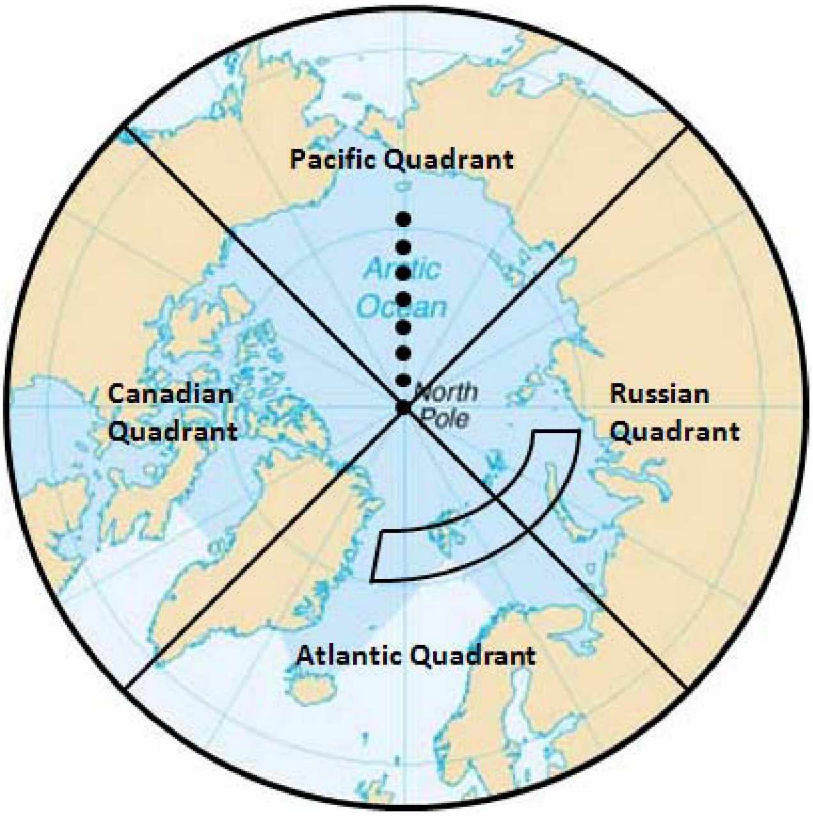

Figure 1.2 Study quadrants, wind sampling, and SST sampling points. Quadrant divisions are shown by black longitudinal lines, and the labels explain where each quadrant is. The 8 dots starting at the North Pole, and continuing to 72.5°N in the Pacific identify points where wind data were sampled. The rounded box in the Atlantic and Russian quadrants depicts the sub-region from which SSTs were analyzed.

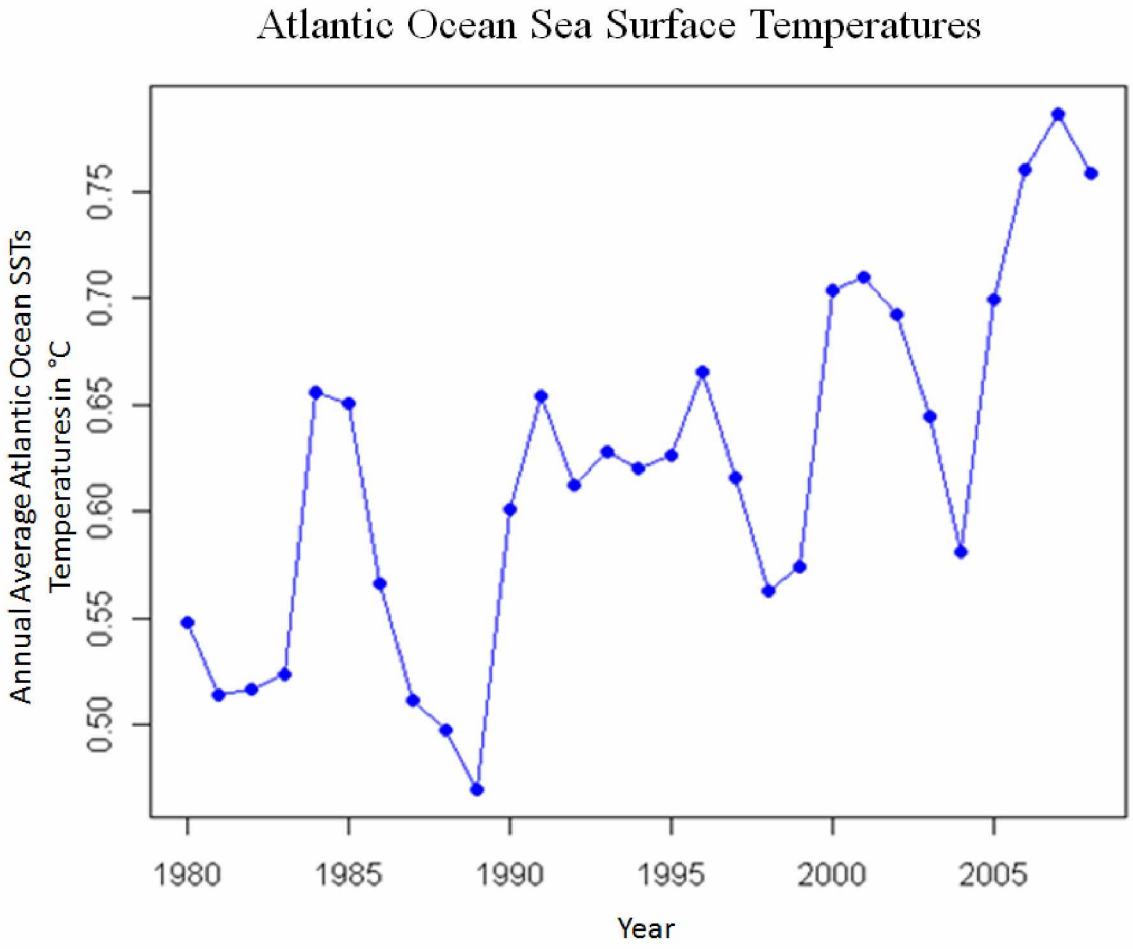

Figure 1.3 Atlantic Ocean SSTs. SST (°C) averaged over 75°-80°N, 20°W-70°E for the 12 months ending in February of the indicated year for 1980-2008. For example, 1990 is calculated as March of 1989 through February of 1990.

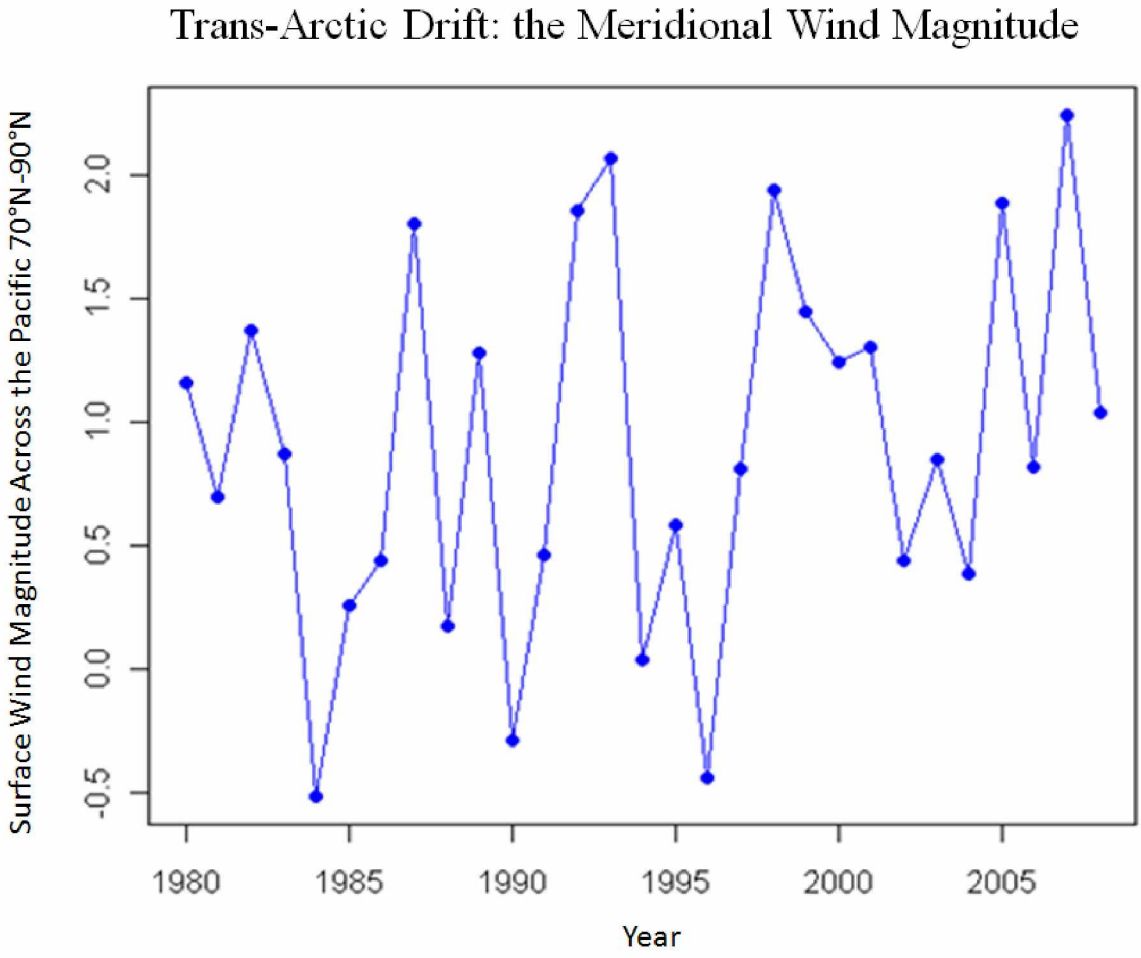

Figure 1.4 Trans-Arctic drift: the meridional wind magnitude. Average wind magnitude from 70N to 90N along the 180 Meridian (points shown in Fig. 1) for June-July. Positive wind magnitudes represent winds blowing from the Pacific towards the North Pole, whereas negative values represent winds blowing away from the North Pole. While the values are scattered year by year, most of the results are positive, which means that winds mostly blow from the Pacific towards the North Pole.

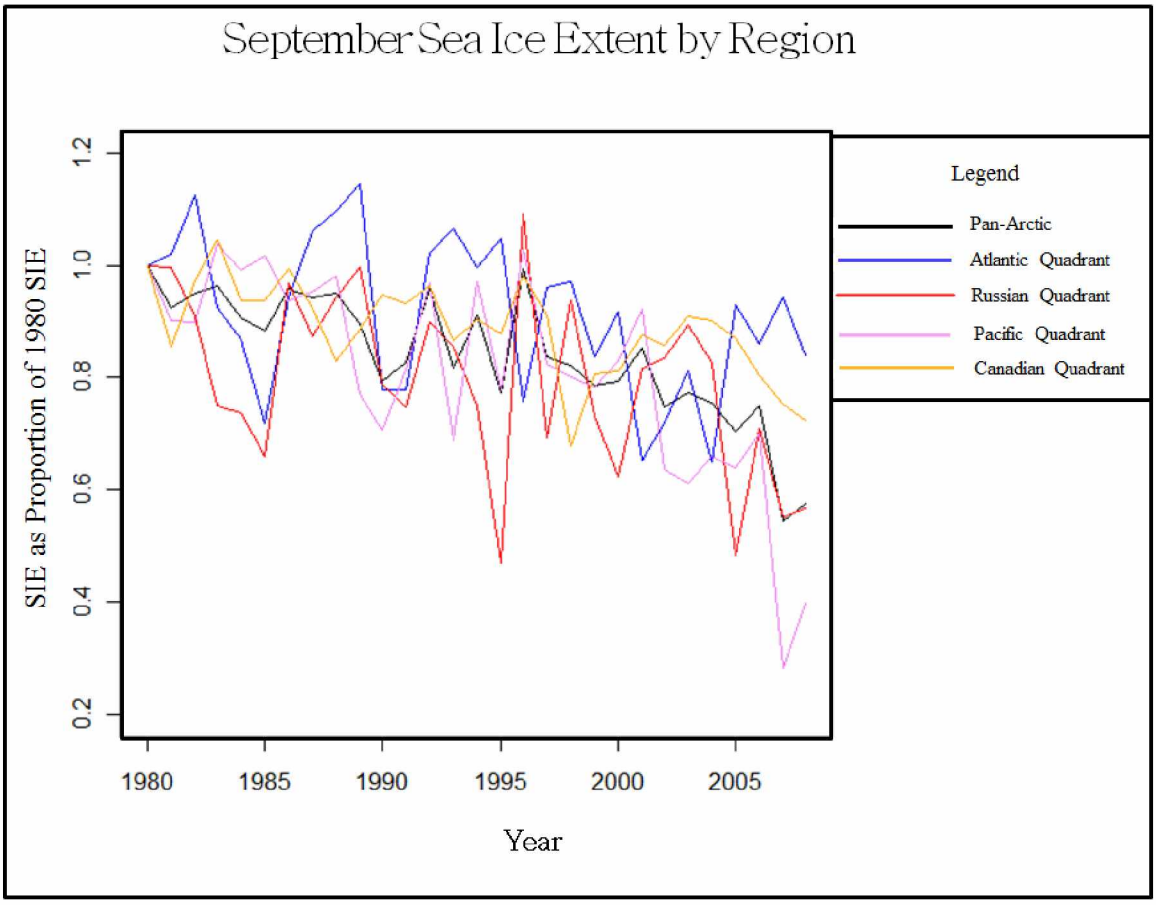

Figure 1.5 September SIE by region, 1980-2008. The colors on the right side correspond to the colors of the different domains on the graph. The highlights of this graph are that Atlantic and Canadian quadrant SIE are decreasing much slower than pan-Arctic trend, while Pacific SIE is decreasing much faster than the pan-Arctic Trend. The Russian quadrant has been decreasing similar to pan-Arctic trend.

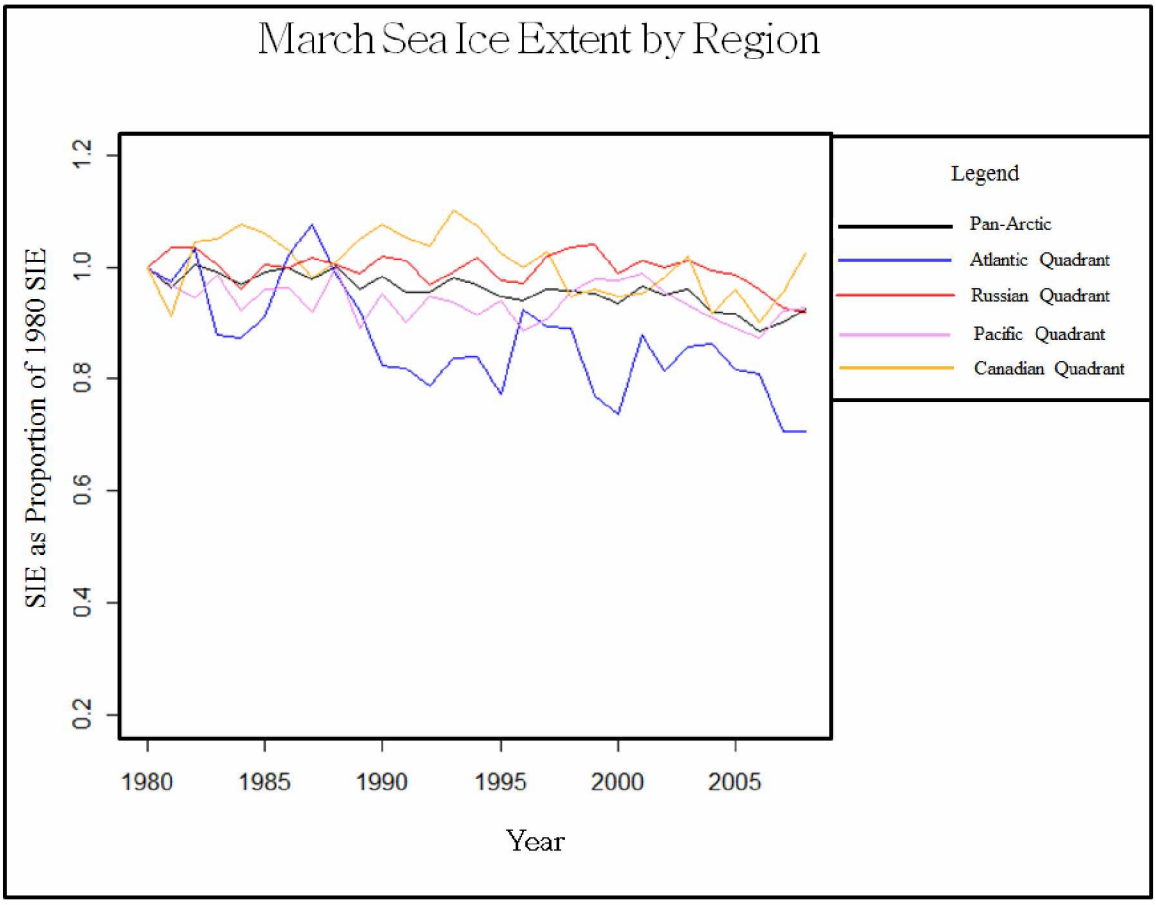

Figure 1.6 March SIE by region, 1980-2008. The colors on the right side correspond to the colors of the different domains on the graph. The highlights of this graph are that the Canadian, Pacific, and Russian quadrants all closely followed the pan-Arctic trend for March SIE loss, while the Atlantic quadrant lost sea ice at a much faster rate.

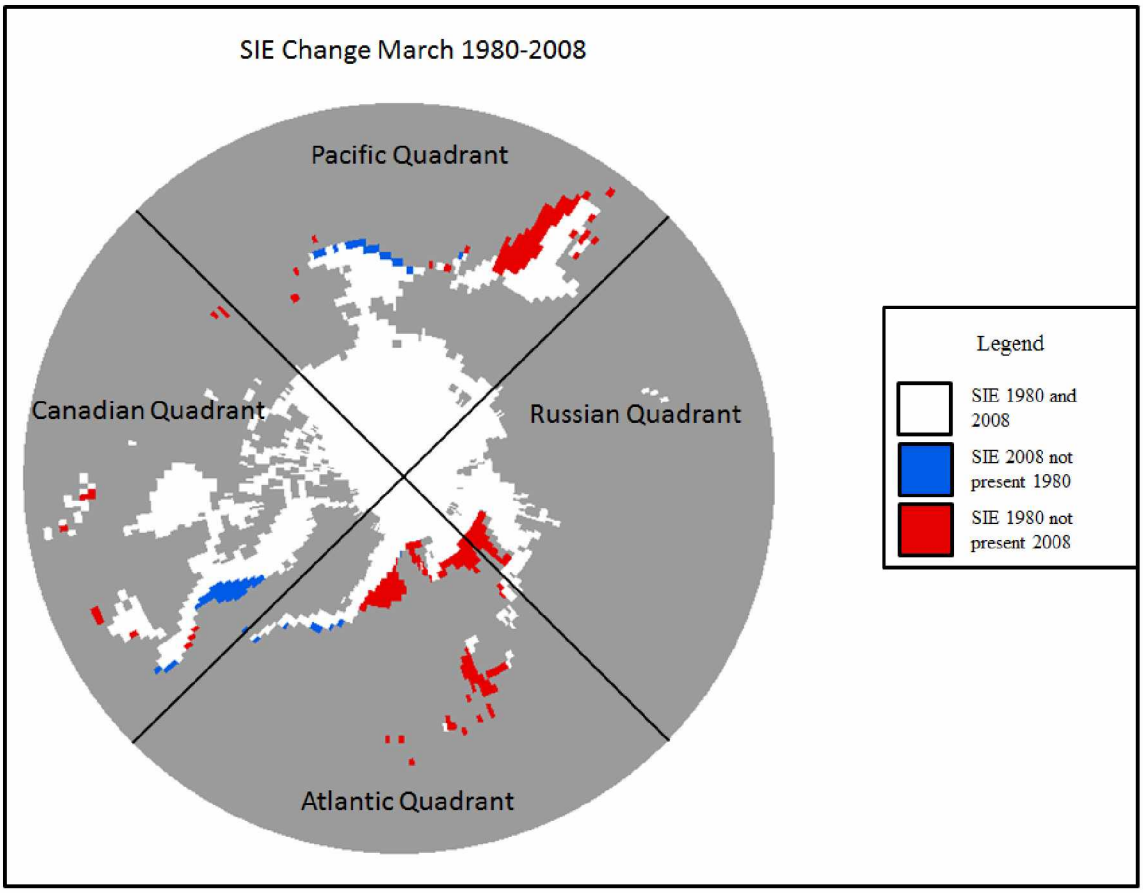

Figure 1.7 SIE change, March, 1980-2008. White represents sea ice present in both years. Red represents sea ice present only in 1980. Blue represents sea ice present only in 2008. The black lines separate the four quadrants.

1.8 References

ACIA, 2005. Arctic Climate Impact Assessment. Cambridge University Press. 1024p. http://www.acia.uaf.edu. Accessed July 26, 2011.

Alexander, M., Bhatt, U., Walsh, J., Timlin, M., Miller, J., and Scott, J. 2004. The atmospheric response to realistic Arctic sea ice anomalies in an AGCM during winter. Journal of Climate. Vol. 17(5). 890-905.

Barber, D., Lukovich, J., Keogak, J., Baryluk, S., Fortier, L., and Henry, G. 2008. The Changing Climate of the Arctic. Arctic. Vol. 61 (Supplement). 7-26.

Budikova, D. 2009. Role of Arctic sea ice in global atmospheric circulation: a review. Global and Planetary Change. Vol. 68(3): 149-163.

Cavalieri, D., Parkinson, C., Gloersen, P., and Zwally, H. 1996, updated 2008. Sea ice concentrations from Nimbus-7 SMMR and DMSP SSM/I passive microwave data, [1980-2007]. Boulder, CO USA: National Snow and Ice Data Center. Digital Media.

Comiso, J., Parkinson, C., Gersten, R., and Stock, L. 2008. Accelerated decline in the Arctic sea ice cover. Geophysical Research Letters 35, L01703, doi: 10.1029/2007GL031972.

Fetterer, F., Knowles, K., Meier, W., and Savoie, M. 2009. Sea Ice Index. Boulder, Colorado USA: National Snow and Ice Data Center. Digital Media.

Francis, J., and Hunter, E. 2007. Drivers of declining sea ice in the Arctic winter: A tale of two seas. Geophysical Research Letters 34, l17503, doi: 10.1029/2007GL030995.

IPCC. 2007. Climate change 2007: the physical science basis—contribution of Working Group I to the Fourth Assessment Report. Cambridge: Cambridge University Press.

Kalnay, E., Kanamitsu, M., Kistler, R., Collins, W., Deaven, D., Gandin, L., Iredell, M., et. al. 1996: The NCEP/NCAR 40-Year Reanalysis Project. Bulletin of the American Meteorological Society: 77, pp. 437-472.

Kauker, F., Gerdes, R., Karcher, M., and Köberle, C. 2005. Impact of North Atlantic Current changes on the Nordic Seas and the Arctic Ocean. Journal of Geophysical Research 110(C12002).

Maslowski, W., Kinney, J., and Jakacki, J. 2007. Toward prediction of environmental arctic change. Computing in Science and Engineering. Vol. 9 (6). 29-34.

Maslowski, W, Kinney, J., Jakacki, J., and Zwally, J. 2008. State of the Arctic sea ice. Geophysical Research Abstracts. Vol. 10.

Meier, W., Fetterer, F., Knowles, K., Meier, W., Savoie, M., and Brodzik, M. 2006, updated quarterly. Sea ice concentrations from Nimbus-7 SMMR and DMSP SSM/I passive microwave data [2008]. Boulder, CO USA: National Snow and Ice Data Center. Digital media.

Meier, W., Stroeve, J., and Fetterer, F. 2007. Whither Arctic sea ice? A clear signal of decline regionally, seasonally, and extending beyond the satellite record. Annals of Glaciology 46. 428-434.

Ogi, M., and Wallace, J. 2007. Summer minimum Arctic sea ice extent and the associated summer atmospheric circulation. Geophysical Research Letters 34, L12705, doi: 10.1029/2007GL029897.

Ogi, M., Rigor, I., McPhee, M., and Wallace, J. 2008. Summer retreat of Arctic sea ice: Role of summer winds. Geophysical Research Letters 35, L24701, doi: 10.1029/2008GL035672.

Ogi, M., Yamazaki, K., and Wallace, J. 2010. Influence of winter and summer surface wind anomalies on summer Arctic sea ice extent. Geophysical Research Letters 37, L07701, doi: 10.1029/2009GL042356.

Overland, J., and Wang, M. 2010. Large-scale atmospheric circulation changes associated with the recent loss of Arctic sea ice. Tellus, 62A, 1-9.

Parkinson, C., and Cavalieri, D. 2008. Arctic sea ice variability and trends, 1979-2006. Journal of Geophysical Research, 113, doi: 10.1029/2007JC004558.

Parkinson, C, Cavalieri, 2., Gloersen, P., Zwally, H., and Comiso, J. 1999. Arctic sea ice extents, areas, and trends, 1978-1996. Journal of Geophysical Research, 104, doi: 10.1029/1999JC9000082.

Polyakov, I., Beszcyczynska, A., Carmack, E., Dmitrenko, I., Fahrbach, E., Frolov, I., Gerdes, R., et. al. 2005. One more step toward a warmer Arctic, Geophysical Research Letters 32, L17605, doi: 10.1029/2005GL023740.

Richter-Menge, J., and Overland, J., Eds. 2010: Arctic Report Card 2010. http://www.arctic.noaa.gov/reportcard. Accessed July 26, 2011.

Rodrigues, J. 2009. The increase in the length of the ice-free season in the Arctic. Cold Regions Science and Technology. Vol. 59 (1). 78-101.

Shein, K., ed. 2006. State of the climate in 2005. Bullet of the American Meteorological Society, 87, S1-102.

Shimada, K., Kamoshida, T., Itoh, M., Nishino, S., Carmack, E., McLaughlin, F., Zimmerman, S., Proshutinsky, A. 2006. Pacific Ocean inflow: Influence on catastrophic reduction of sea ice cover in the Arctic Ocean. Geophysical Research Letters, 33. doi: 10.1029/2005GL025624.

Stroeve, J., Holland, M., Meier, W., Scambos, T., and Serreze, M. 2007. Arctic sea ice decline: Faster than forecast. Geophysical Research Letters 34, L095101, doi: 10.1029/2007GL029703.

Timmermans, M, Francis, J., Proshutinsky, A., Hamilton, L. 2009. Taking stock of arctic sea ice and climate. American Meteorological Society. Vol. 90 (9). 1351-1353.

Walsh, J., Chapman, W., Romanovsky, V., Christensen, J., and Stendel, M. 2008. Global Climate Model Performance over Alaska and Greenland. Journal of Climate. Vol. 21 (23). 6156-6174.

Wang, M. and Overland, J. 2009. A sea ice free summer Arctic within 30 years? Geophysical Research Letters. Vol. 36, L07502, doi: 10.1029/2009GL037820

Zhang, X. 2010. Sensitivity of Arctic summer sea ice coverage to global warming forcing: towards reducing uncertainty in Arctic climate change projections. Tellus: Series A. Vol. 62 (3). 220-227.

Zhang, X., and Walsh, J. 2006. Toward a seasonally ice-covered Arctic Ocean: scenarios from the IPCC AR4 model simulations. Journal of Climate 19. 1730-1747.

CHAPTER 2

AN EVALUATION OF GLOBAL CLIMATE MODELS: ARCTIC SEA ICE EXTENT

2.1 Abstract

This study evaluated the performance of 13 Global Climate Models, analyzing retrospective simulations for sea ice extent from 1980 through 2008, using three performance metrics: the September trend, the March trend, and the seasonal cycle of monthly mean sea ice extent. We evaluated model performance pan-Arctic and within four longitude-based quadrants (Atlantic, Russian, Pacific and Canadian). Our results suggest variations in the accuracy of individual model simulations across regions; a few in particular stand out for overall performance: Hadley Gem1, Miroc 3.2 Medium Resolution, the Institute for Numerical Mathematics CM3, and the Goddard Institute for Space Studies Model AOM. While past performance does not guarantee that a model will perform well in the future, the models that best capture recent sensitivities of sea ice must be considered strong candidates for use in projecting future sea ice responses to externally forced climate change.

2.2 Background

Climate models inadequately portray the speed with which SIE is diminishing in the Arctic (Stroeve et al., 2007). Shortcomings with the current range of forecasts underscore the importance of understanding Atmosphere Ocean General Circulation Models (AOGCM). At the release of AR4, scientists predicted an ice-free summer sea towards the end of this century based on model simulations; after analyzing the limitations of the sea ice output and the current rate of sea ice decline, several groups have estimated an ice free summer earlier than 2050 (Stroeve et al., 2007; Comiso et al., 2008; Wang and Overland, 2009). Comparison of performance between models offers a guide to those models' potential for capturing the effects of changes in atmospheric and oceanic forcing. Improving sea ice models will be of critical importance in providing the information required to develop sound management strategies and informed policy (AMSA, 2009). Further, this translates into a greater scientific understanding of changing ecosystems, empowering individuals, communities, and societies to adapt to impacts of climate change.

While several studies have evaluated SIE simulation performance in climate models (e.g. Zhang and Walsh, 2006; Wang and Overland, 2009), only Overland and Wang (2007) have analyzed regional variations in the Arctic. However, our analysis uses different regional divisions and uses a different rating system than Overland and Wang. The objective of this study is to evaluate the performance of AOGCMs' capability to simulate SIE for the period 1980 through 2008 in the Arctic and its sub-regions.

2.3 Data and Methods

Observed SIE data from 1980 to 2008 come from the National Snow and Ice Data Center's (NSIDC) passive microwave data set (Cavalieri et al., 1996; Meier et al., 2006). These data are comprised of four sets of satellite data: Nimbus-7 SMMR (January 1980 - August 1987), DMSP-F8 SSM/I (July 1987 - December 1991), DMSP-F11 SSM/I (December 1991 – September 1995), and DMSP-F13 SSM/I (May 1995 – Current). Sea ice concentrations come from a revised NASA Team algorithm (Cavalieri et al., 1996).

Model performance was assessed for pan-Arctic SIE and four quadrants: 46° W to 45° E (Atlantic), 46° E to 135° E (Russian), 136° E to 135° W (Pacific), and 136° W to 45° W (Canadian). This is based on the division used in the ACIA (2005). The AOGCMs used in this research were forced with the A1B emissions scenario. At the release of AR4, A1B was a middle-of-the-road scenario for emissions. Since that report, global emissions of greenhouse gases have exceeded all emission scenarios from AR4. Higher emissions are expected to result in more climate forcing than prescribed in these models (IPCC, 2007; Solomon et al., 2009). However, the AOGCMs used observed GHG concentrations for 1980-2000. Since this study covers 1980-2008; 2001-2008 use the A1B emissions scenario (IPCC, 2007; UNMDG, 2010), and all forcing scenarios are very similar during this period.

Simulated SIE for 13 models (Table 2.1) for the historical period 1980-2008 was compared to the observed satellite record to develop a performance ranking. The performance ranking measures accuracy of each model based on three metrics: September SIE trend, March SIE trend, and the annual cycle of SIE. The first two metrics were analyzed using a least squares linear regression time series for March and September SIE. The difference between the slope of the regression line for the model output and the observed record is used to rank the March and September trends. The third performance metric compares observed SIE for each month from 1980-2008 to a model's simulated SIE. For example, in the month of January, an average is produced from 1980-2008 for both the model and the observed record. Once all months have been compared in this manner, the average of the absolute value of these differences is calculated. This metric evaluates a model's annual cycle of SIE, while averaging natural year to year variation. Each model earns a rank for each metric from 1-13, which is summed to create a composite rank. In this case, a smaller number represents a better rank for the model. These methods were repeated for regional SIE performance to determine which models perform best in each of the four quadrants. The rankings from the four quadrants were also summed to create a combined quadrants rank.

2.4 Results

Table 2.2 presents the pan-Arctic performance of models. The models that performed best for the September trend simulated the greatest decrease in September. Only one model, INM, had a more rapid trend in September than the observed record. All other models underestimated the September trend. CCSM showed a more rapid rate of decline in March than the observed record, while all other models underestimated the March trend (Table 2.2). Full performance results by region are in Table 2.3.

A Spearman rank-order correlation test indicated that most regions had correlated ranks (Table 2.4). The pan-Arctic results positively correlated with all regions, although the correlations with the Atlantic and Russian quadrants were weak. The combined quadrant had high correlations with all but the Russian quadrant.

A number of major studies have evaluated AOGCMs in the Arctic, and as part of this study we compared results across all evaluations (Table 2.5). However, individual methods vary. Zhang & Walsh (2006) and Arzel et al. (2006) selected models that simulated annual SIE within 10 percent of the observed record from 1979-1999. Overland and Wang (2007) selected models that simulated annual SIE within 20 percent from 1979-1999. Walsh et al. (2008), the only study here that did not investigate SIE, evaluated models based on their assessment of several climatic variables and developed a composite rank for each model. Wang and Overland (2009) selected models that simulated September SIE within 20 percent from 1979-1999. Zhang (2010) selected model runs that performed best in sea ice sensitivity tests to change in temperature from 1979-2004. A comparison of model performance across the studies finds that MRCM is the most consistent model, while HADGEM is the second most consistent model (Table 2.5).

Overland and Wang (2007) is the only other SIE model evaluation that investigated regional performance of SIE models. Since their regions were based on Arctic seas, as opposed to longitudinal regions, we merged their regions to fit our quadrants. The resultant comparison identified many similarities between the two studies (Table 2.6).

We compared the four best performing pan-Arctic models to the remaining nine models (Fig. 2.1). While the points for the four model mean are scattered, their trend line is much closer to the observed record's trend line than that of the remaining nine models. Extending the top five pan-Arctic models into the future reveals a range of future sea ice scenarios (Fig. 2.2).

2.5 Conclusions

AOGCM performance evaluation identified the models that most accurately simulated SIE from 1980-2008. Depending on the evaluation region, model performance rank differed. The pan-Arctic region and combined quadrants shared three of the same best performing models: HADGEM, MRCM and INM. INM remained in the top five for all six tests. MRCM remained in the top five for five of the six tests. GISS and HADGEM remained in the top five for four of the six tests. When investigating pan-Arctic SIE, HADGEM out-performed the other models, ranking first in two metrics, and third in the other, which resulted in a low composite rank. Based on these analyses, MRCM, INM, HADGEM, and GISS are the best performing models.

In evaluating pan-Arctic sea ice, a model could project much higher SIE in one region but much lower in another region, still resulting in strong performance. Thus if the aim is to investigate a specific region's SIE, the best performing regional projections should be used. For example, HADGEM ranked last in the Russian quadrant and in the bottom half in the Canadian quadrant, while being best in pan-Arctic, and second in the Atlantic quadrant.

Furthermore, the composite does not weigh quadrants according to quantity of sea ice; in the winter, the Pacific quadrant has more than double the sea ice of either the Atlantic or Canadian quadrants. For these reasons, neither approach is necessarily better when selecting models for pan-Arctic simulations. However, in pan-Arctic simulations that require accurate portrayal of regional SIE, the models that performed best in the combined quadrants may be the better choice.

Investigating individual properties of models revealed that the top performing models in this study, INM, MRCM, GISS, and HADGEM all have similar characteristics. All four have natural forcing in 20C3M. Three did not use flux adjustments, whereas INM only used flux adjustments for a few regions. For sea ice physics, HADGEM and MRCM used elastic-viscous plastic rheology, and GISS used viscous-plastic rheology. HADGEM and INM used a thickness distribution, although neither MRCM nor GISS did. Three of the poorest performing models, CSIRO, CCCMA, and HAD did not share many characteristics with the best performing models. None of the lowest-ranked models used natural forcing in 20C3M. For sea ice physics, CCCMA and CSIRO used cavitating fluid, while HAD used drifting by ocean currents. CCCMA used heat and water flux adjustments. More sophisticated sea ice physics and natural forcing in 20C3M appear to have an effect on the performance of sea ice models. This study did not find that spatial resolution had a significant effect on sea ice output; however, some sea ice characteristics will require finer resolution, such as coastal interactions, salinity, and thickness (IPCC Model Documentation, 2007)

Using an evaluative approach for AOGCM performance is important when analyzing future sea ice scenarios, particularly if the intention is to investigate local or regional sea ice dynamics. These rankings can therefore be used as guidelines for model selection when investigating future projections. However, AOGCMs use many assumptions that may not hold into the future. The use of emissions scenarios is a leading uncertainty – global greenhouse gas emissions could increase well beyond the highest emissions scenarios, or dip below the lowest.

ACIA designed longitude-based regional divisions to study the human dimensions of climate change. For their evaluation of climate models, Overland and Wang (2007) used the regional division designed by Parkinson et al. (1999), which followed the physical designations of Arctic seas. Both of these approaches to evaluating regional SIE are valid, but we chose to investigate climate model performance based on the longitudinal approach developed by ACIA. Our study is the first to utilize the ACIA division for the purpose of evaluating AOGCM performance of SIE. Similar to other

evaluative studies (Arzel et al., 2006; Zhang and Walsh, 2006; Stroeve et al., 2007; Wang and Overland, 2009; Zhang, 2010), this research indicates that sea ice changes are occurring faster than almost any model simulations, particularly from 2000-2008.

Figure 2.3 shows a broad range of model projections for the 21st century. By narrowing those models to consideration of best performers, we identify a smaller range of future scenarios (Zhang, 2010). Figure 2.2 shows a subset of models based on their performance in this study. Compared to Figure 2.3, it shows a more rapid retreat of SIE by 2100. A subset of models may narrow the range of projected changes, which may reduce uncertainty in future scenarios. A subset will also reduce information on distribution and possible extreme scenarios. Recent research suggests that observed SIE trends are outpacing modeled trends, and that even extreme SIE decline already has exceeded model projections (Stroeve et al., 2011). Improving model performance for SIE will aid development of more accurate global climate change projections.

2.6 Tables

Table 2.1 The models evaluated in this study.

Acronym	Organization	Model Name	Country
BCCR	Bjerknes Centre for Climate Research	BCM 2.0	Norway
CCSM	National Center for Atmospheric Research	Community Climate System Model 3.0	USA
CCCMA	Canadian Centre for Climate Modelling and Analysis	Coupled General Circulation Model 3.1	Canada
CNRM	Météo-France and Centre National de Recherches Météorologiques	CM3	France
CSIRO	Commonwealth Scientific and Industrial Research Organisation	Mark Version 3.0	Australia
ECH	Max Planck Institute for Meteorology	ECHAM5/MPI-OM	Germany
GISS	Goddard Institute for Space Studies	Model AOM	USA
HAD	Hadley Centre for Climate Prediction and Research and the Met Office	CM3	UK
HADGEM	Hadley Centre for Climate Prediction and Research and the Met Office	GEM1	UK
INM	Institute for Numerical Mathematics	INM-CM 3.1	Russia
IPSL	L'Institut Pierre-Simon Laplace	Couple Model CM4	France
MRCM	Center for Climate System Research, National Institute for Environmental Studies, and Frontier Research Center for Global Change	MIROC3.2 medium-resolution	Japan
MRI	Meteorological Research Institute	Couple General Circulation Model 2.3.2	Japan

Table 2.2 Pan-Arctic model performance. The September and March trends are measured in square kilometers per year. The annual cycle is in square kilometers. The top row displays the observed satellite record and subsequent rows show the output for each model.

	September Trend, km^2/yr	March Trend, km^2/yr	Annual Cycle km^2
Observed	-82240	-46432	----------
BCCR	-13805	-24635	777894
CCCMA	-17613	-3132	898971
CCSM	-65535	-51082	809307
CNRM	-28546	31630	932108
CSIRO	-12608	-5051	802664
ECH	-24273	-19208	748364
GISS	-17629	-9453	733971
HAD	-46729	-18474	892375
HADGEM	-77914	-43675	716300
INM	-88593	-17312	713620
IPSL	-41484	-29982	754628
MRCM	-40514	-30824	682600
MRI	-10637	-23215	731048

Table 2.3 GCM Performance. The composite ranks of models evaluated in this study, by study region. The models' order follows pan-Arctic ranking. Each model earns a rank for each metric from 1-13, which is summed to create a composite rank. The first number in each column shows the rank of each model within that region; the number in parentheses is the composite rank.

	Pan-Arctic	Atlantic	Russian	Pacific	Canadian	Combined Quadrants
HADGEM	1 (5)	2 (9)	13 (28)	3 (16)	8 (25)	4 (78)
MRCM	2 (10)	10 (27)	6 (20)	4 (17)	1 (3)	2 (67)
INM	3 (13)	1 (18)	4 (19)	1 (14)	2 (14)	1 (55)
CCSM	4 (15)	13 (32)	9 (25)	11 (26)	8 (25)	13 (108)
IPSL	5 (16)	7 (23)	7 (23)	1 (14)	10 (26)	6 (86)
ECH	6 (21)	11 (28)	1 (10)	12 (27)	6 (24)	9 (89)
HAD	7 (23)	8 (25)	9 (25)	7 (21)	4 (15)	6 (86)
MRI	7 (23)	3 (10)	4 (19)	9 (24)	11 (27)	5 (80)
BCCR	9 (24)	5 (19)	8 (24)	6 (19)	6 (24)	6 (86)
GISS	9 (24)	4 (18)	9 (25)	5 (18)	2 (14)	3 (75)
CSIRO	11 (32)	6 (20)	12 (26)	10 (25)	13 (32)	12 (103)
CNRM	12 (33)	8 (25)	3 (15)	7 (21)	12 (28)	9 (89)
CGCM	13 (34)	12 (29)	2 (14)	13 (31)	5 (16)	11 (90)

Table 2.4 Spearman Rank-Order Correlation Coefficient. A positive proportion indicates correspondence of ranks across sectors; near-zero or negative values do not.

	Atlantic	Russian	Pacific	Canadian	Combined
Pan-Arctic	.25	.16	.45	.47	.61
Atlantic	----------	-.3	.64	-.02	.67
Russian	----------	----------	-.28	.12	-.02
Pacific	----------	----------	----------	.27	.78
Canadian	----------	----------	----------	----------	.59

Table 2.5 Model evaluation synthesis. This table synthesizes model performance over several studies. An x (upper or lower case) indicates that the model performed well in that study. A lower case x indicates the model performed in the lowest ranked three models in either our combined quadrants or pan-Arctic evaluation. Bold indicates the model performed in the best five models in our pan-Arctic evaluation. Underlines indicate the model performed in the best five models in our combined quadrants evaluation.

	Pan-Arctic	Combined Quadrants	Zhang & Walsh 2006	Arzel et al. 2006	Walsh et al. 2008	Overland & Wang 2007	Wang & Overland 2009	Zhang 2010
BCCR								
CCCMA			x	x		x		
CCSM	**x**					**x**	**x**	**x**
CNRM				x	x		x	x
CSIRO			x					
ECH					X	X		X
GISS		X	X	X		X		
HAD			X		X			
HADGEM	**X**	**X**				**X**	**X**	**X**
INM	**X**	**X**						
IPSL	**X**			**X**			**X**	**X**
MRCM	**X**	**X**	**X**	**X**	**X**	**X**	**X**	**X**
MRI		X						

Table 2.6 Regional evaluation comparison. A comparison between the results of Overland and Wang (2007) and the present study. The regions from Overland and Wang were fit to the quadrants from this study, and models that performed well in those quadrants are marked with an X. Bold shows that the model also performed well in this study.

	Atlantic	**Russian**	**Pacific**	**Canadian**
BCCR				**X**
CCSM	X	**X**	X	**X**
CCCMA		X	X	X
CNRM				X
CSIRO				X
ECH	X	**X**	X	X
GISS	**X**	X	**X**	**X**
HAD				**X**
HADGEM	**X**	**X**	**X**	X
INM	**X**	**X**		
IPSL		X	**X**	X
MRCM			**X**	**X**
MRI	**X**	**X**		X

2.7 Figures

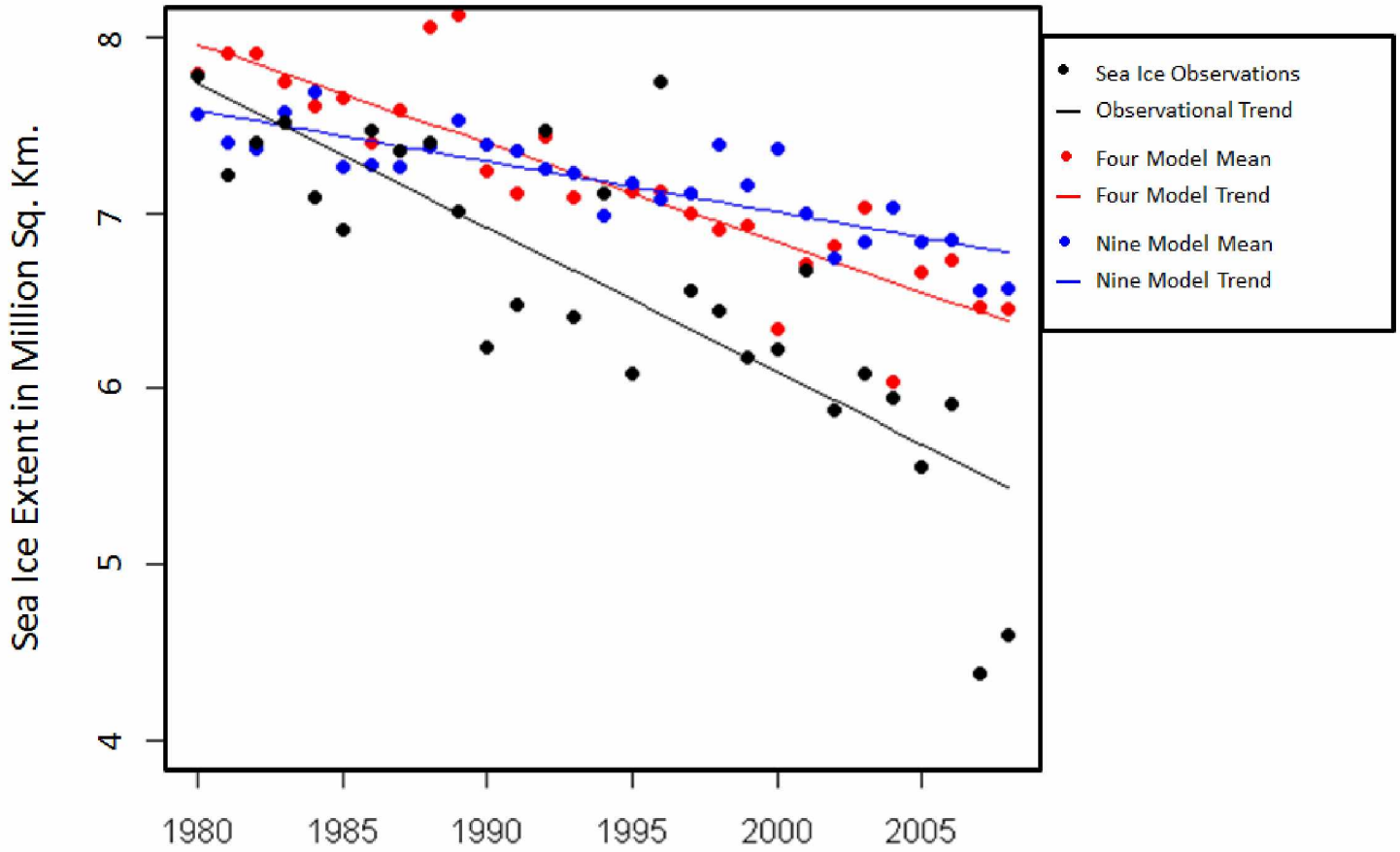

Figure 2.1 Projected vs. observed September SIE. September ice extent from 1980-2008 for the mean of four best performing models in red, the observed SIE in black, and the mean of the remaining nine models in blue.

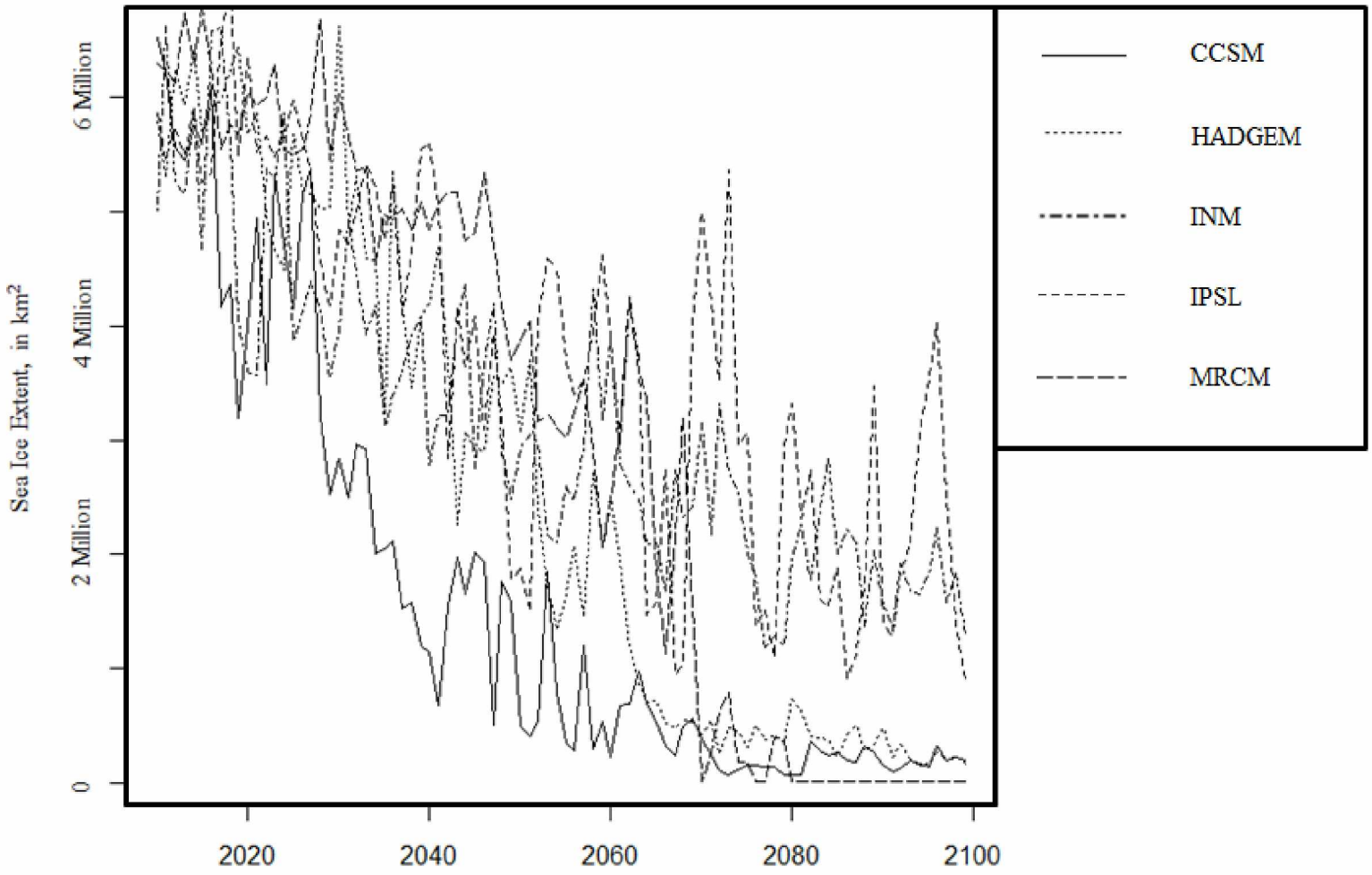

Figure 2.2 Pan-Arctic SIE projections, September 2010-2100. Models used include CCSM, HADGEM, INM, IPSL, and MRCM

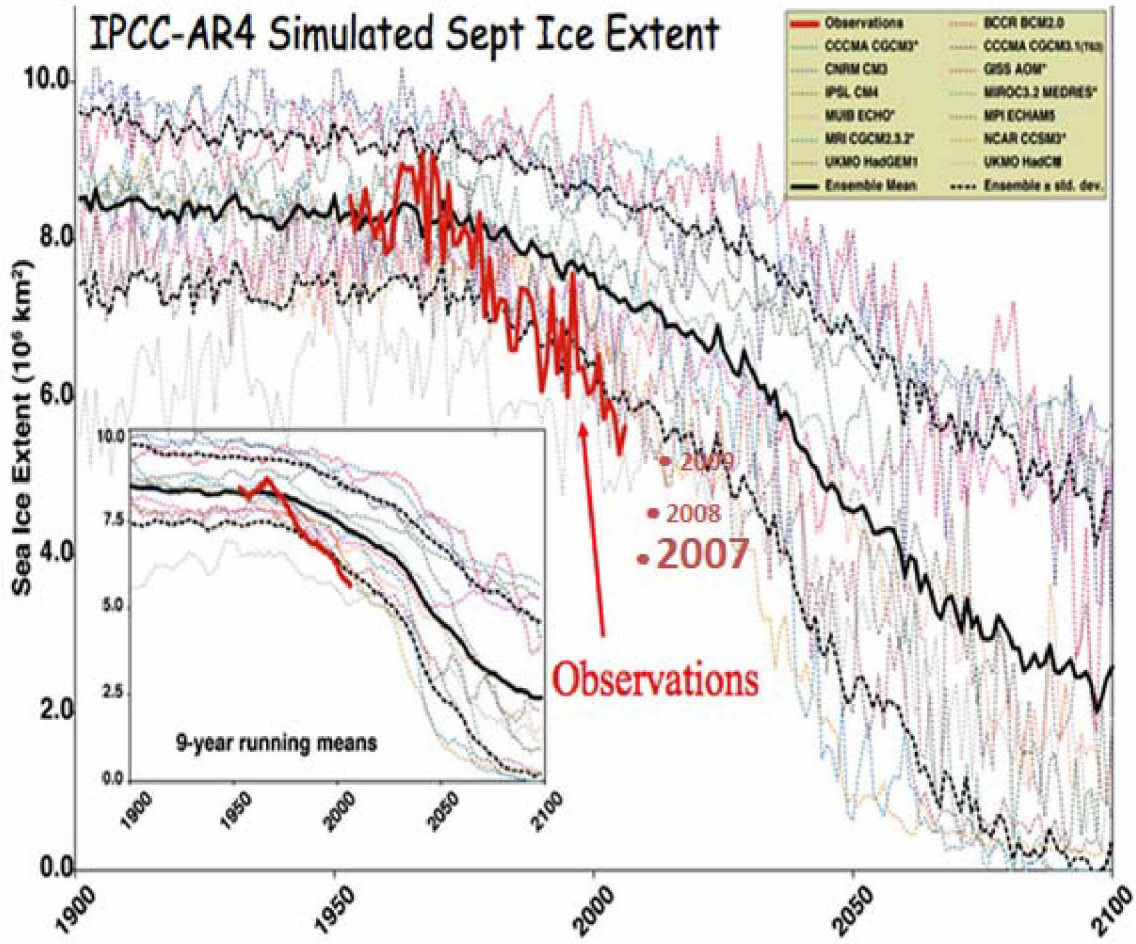

Figure 2.3 IPCC-AR4 simulated September SIE from Stroeve et al. (2007). Simulations from AOGCMs are in the indicated style and color, whereas the observations are solid red.

2.8 References

ACIA, 2005. Arctic Climate Impact Assessment. Cambridge University Press. 1024p. http://www.acia.uaf.edu Accessed. July 26, 2011.

AMSA. 2009. Arctic Marine Shipping Assessment 2009 Report. Arctic Council, April 2009. http://www.pame.is/amsa. Accessed July 26, 2011.

Arzel, O., Fichefet, T., and Goosse, H. 2006. Sea ice evolution over the 20th and 21st centuries as simulated by current AOGCMs. Ocean Modelling 12 (2006) 401-415.

Boé, J., Hall., A., and Qu, X. 2009. September sea-ice cover in the Arctic Ocean projected to vanish by 2100. Nature Geoscience. doi: 10.1038/NGEO467.

Cavalieri, D., Parkinson, C., Gloersen, P., and Zwally, H. 1996, updated 2008. Sea ice concentrations from Nimbus-7 SMMR and DMSP SSM/I passive microwave data, [1980-2007]. Boulder, CO USA: National Snow and Ice Data Center. Digital Media.

Comiso, J., Parkinson, C., Gersten, R., and Stock, L. 2008. Accelerated decline in the Arctic sea ice cover. Geophysical Research Letters 35, L01703, doi: 10.1029/2007GL031972.

IPCC. 2007. Climate change 2007: the physical science basis—contribution of Working Group I to the Fourth Assessment Report. Cambridge: Cambridge University Press.

IPCC Model Documentation. 2007. CMIP3 climate model documentation, references, and links. Intergovernmental Panel on Climate Change. http://www-pcmdi.llnl.gov/ipcc/model_documentation/ipcc_model_documentation.php. Accessed July 26, 2011.

Meier, W., Fetterer, F., Knowles, K., Meier, W., Savoie, M., and Brodzik, M. 2006, updated quarterly. Sea ice concentrations from Nimbus-7 SMMR and DMSP

SSM/I passive microwave data [2008]. Boulder, CO USA: National Snow and Ice Data Center. Digital media.

NSIDC. 2010. Arctic sea ice falls to third-lowest extent. National Snow and Ice Data Center, 10-4-2010. http://www.nsidc.org/news/press/20101004_minimumpr.html. Accessed July 26, 2011.

Overland, J., and Wang, M. 2007. Future regional Arctic sea ice declines. Geophysical Research Letters 34. doi: 10.1029/2007GL030808.

Parkinson, C, Cavalieri, 2., Gloersen, P., Zwally, H., and Comiso, J. 1999. Arctic sea ice extents, areas, and trends, 1978-1996. Journal of Geophysical Research, 104, doi: 10.1029/1999JC9000082.

Solomon, S., Plattner, G., Knutti, R., and Friedlingstein, P. 2009. Irreversible climate change due to carbon dioxide emissions. Proceedings of the National Academy of Sciences of the United States of America. doi: 10.1073/pnas.081221106.

Stroeve, J., Holland, M., Meier, W., Scambos, T., and Serreze, M. 2007. Arctic sea ice decline: Faster than forecast. Geophysical Research Letters 34, L095101, doi: 10.1029/2007GL029703.

Stroeve, J., Serreze, M., Holland, M., Kay, J., Malanik, J., and Barret, A. 2011. The Arctic's rapidly shrinking sea ice cover: a research synthesis. Climatic Change. doi: 10.1007/s10584-011-0101-1.

Timmermans, M., Francis, J., Proshutinsky, A., Hamilton, L. 2009. Taking stock of arctic sea ice and climate. American Meteorological Society. Vol. 90 (9). 1351-1353.

UNMDG. 2010. United Nations Statistics Division, Millennium Development Goals indicators: Carbon dioxide emissions (CO2). http://mdgs.un.org/unsd/mdg/SeriesDetail.aspx?srid=749&crid=. Accessed July 26, 2011.

Walsh, J., Chapman, W., Romanovsky, V., Christensen, J., and Stendel, M. 2008. Global Climate Model Performance over Alaska and Greenland. Journal of Climate. Vol. 21 (23). 6156-6174.

Wang, M. and Overland, J. 2009. A sea ice free summer Arctic within 30 years? Geophysical Research Letters. Vol. 36, L07502, doi: 10.1029/2009GL037820.

Winton, M. 2011. Do climate models underestimate the sensitivity of Northern Hemisphere sea ice cover? Journal of Climate. doi: 10.1175/2011JCLI4146.1

Zhang, X. 2010. Sensitivity of Arctic summer sea ice coverage to global warming forcing: towards reducing uncertainty in Arctic climate change projections. Tellus: Series A. Vol. 62 (3). 220-227.

Zhang, X., and Walsh, J. 2006. Toward a seasonally ice-covered Arctic Ocean: scenarios from the IPCC AR4 model simulations. Journal of Climate 19. 1730-1747.

CHAPTER 3

FUTURE ARCTIC SEA ICE DYNAMICS AND IMPLICATIONS FOR MARINE ACCESS

3.1 Abstact

Current sea ice trends and future scenarios suggest that summer sea ice could completely disappear by the end of the 21st century. Over the past decade (2000-2010), sea ice conditions have allowed greater access to the Arctic Ocean by marine transport. We used the models that we identified simulated sea ice extent to examine nine-year mean projections for 2030, 2060, and 2090 and analyze simulated changes in extent of sea ice in the Bering Strait, Northwest Passage, Northeast Passage, and Arctic Bridge. Based on model simulations, all areas will likely experience reduced sea ice coverage over the next century, which would allow ships to operate within a lengthening summer transport season. In particular, the projections for the Northwest Passage and Northeast Passage hold the greatest potential for future access and shipping opportunities. Increased Arctic access brings greater concerns related to search and rescue, environmental risks, and impacts to Indigenous populations in the affected regions, as well as opportunities for resource development and marine access.

3.2 Background

Since 2000, Arctic shipping activity has resulted in a surge of interest in understanding current sea ice conditions and in developing accurate projections. Current sea ice trends and future scenarios suggest that summer sea ice could completely disappear by the end of the 21st century. The Arctic Council investigated Arctic marine access and subsequently released the Arctic Marine Shipping Assessment (AMSA) in 2009.

AMSA stands out for its treatment of Arctic marine issues, but its use of model simulations was limited in scope. This study seeks to expand upon AMSA's scenarios of Arctic marine accessibility by using best performing AOGCMs to analyze future scenarios and identify potential access to the Arctic Ocean by ice-strengthened vessels.

3.3 Data and Methods

Chapter 2 identified models that best simulated sea ice in the Arctic: Hadley Centre Global Environmental Model GEM1 (HadGEM), MIROC Medium Resolution Model (MRCM), Community Climate System Model 3.0 (CCSM), and L'Institut Pierre-Simon Laplace Coupled Model (IPSL). Nine-year means were constructed for each model for 2030, 2060, and 2090 (2026-2034, 2056-2064, 2086-2094). For comparative purposes, a nine-year mean of the observed sea ice record from 2000 through 2008 was computed based on satellite records of sea ice presence in the years under consideration. Interpreting the model output requires some understanding of SIE. When calculating Arctic SIE, the region is divided into pixels based on the desired or available resolution for the dataset. In this case, the resolution for model output for sea ice is one degree latitude by one degree longitude. Any pixel with sea ice concentration of 15 percent or greater is considered to have sea ice present, whereas any pixel with less than 15 percent concentration is classified as not having sea ice present. If a pixel contained sea ice for five or more years, sea ice was considered present for the nine-year mean. For an example of sea ice projections, Figure 3.1 depicts HadGem's nine-year mean for 2026-

2034, as well as the projected SIE for 2026, 2030, and 2034, to illustrate the variations in year to year SIE.

Before investigating individual Arctic routes, we examined the observed and projected SIE. We used a least squares linear regression for a time series of the observed SIE from 1980-2008 and again from 1980-2006. We then fit these time series to future years so we could compare current trends to model projections. We performed this analysis so that the model projections could be compared to current sea ice trends.

We calculated projected Arctic ice-cover, defined as the percent of Arctic seas north of the Arctic Circle that have SIE presence, for every month of 2030, 2060, and 2090. We averaged the projected percentage of cover from the four models. This calculation provides insight to the annual cycle of future SIE decline.

Our study evaluates Arctic marine access for a particular type of vessel, classified according to the Polar Code (PC). The PC, already a voluntary set of guidelines, is a proposed, mandatory system for ships navigating in ice-covered water (Table 3.1). The most capable vessel, PC-1, is a nuclear icebreaking ship capable of handling thick, multiyear ice. A PC-7 vessel is capable in Arctic water, but can only traverse thin, first year ice. In this study, we evaluate the accessibility of the Arctic Ocean to PC-7 vessels. For the purposes of this study, a route can be considered open if the ice edge does not block the route in question. However, in the early stages of ice freeze-up, or during late stages of thaw, a Polar Class 7 vessel is capable of traversing, so some leeway is required when interpreting the results. There is a degree of subjectivity in this study's interpretation of accessibility, and for that reason we have included some model projections (see appendix 3.1).

Since we created nine-year means, these projections represent what might be expected for normal conditions in approximately 2030, 2060, and 2090. However, significant inter-annual variability occurs, such as the extreme minimum SIE of 2007. Inter-annual variability can result in a route opening a month earlier than expected or remaining closed year-round. Therefore, even if these opening and closing dates are

accurate for a mean year, they are not indicative of the range of sea ice conditions that are possible within the time period shown (Fig. 3.1).

The Bering Strait region separates the Pacific and Arctic Oceans between Russia and Alaska. This region has particular significance to the Arctic because it provides the only access point to the Arctic Ocean from the Pacific region. It freezes every winter and thaws every summer, a condition which is expected to continue through 2099 in all model outputs.

The Northeast Passage is defined as a route from the Bering Strait to northern Europe, across the top of Eurasia. Use of a PC-7 vessel on this route requires there be little or no land-fast ice along the north coast of Russia. In recent years, most of the Russian coast becomes free of ice by September, except for the crossing from the Kara Sea to the Laptev Sea. However, transport ships can contract for escort by Russian icebreakers, making the route feasible with PC-7 vessels (Brigham, 2010).

The Northwest Passage "…is the name given to the various marine routes between the Atlantic and Pacific oceans along the north coast of North America that spans the Canadian Arctic Archipelago" (AMSA, 2009: 20). In some areas, the width of the passage is as narrow as 10 kilometers. This means that in the model, as little as two pixels of sea ice portray a blocked passage between Devon and Baffin Islands. As with the Northeast Passage, however, icebreakers can keep the passage open for PC-7 vessels through that short stretch.

The Arctic Bridge, a proposed future shipping route, starts in Murmansk, Russia, crosses the northern Atlantic Ocean, south of Greenland, enters the Hudson Bay, and ends in Churchill, Canada.

3.4 Results

Our linear regression analysis found decreases of 82240 sq. km. per year in the 1980-2008 trend, and 64800 sq. km. per year in the 1980-2006 trend (Table 3.2). The first trend, which included 2007 and 2008, indicated a faster decline of sea ice than projected by the models, whereas the second trend predicted an almost identical SIE to the model

average for 2030, 2060, and 2090. If 2007 and 2008 are considered to be anomalous years, the model means for 2030, 2060, and 2090 are representative of current SIE trends. Given that sea ice in 2009 and 2010 did not recover to pre-2007 levels (Stroeve et al., 2011), 2008 is most likely not an extreme SIE minimum. Therefore, SIE will most likely continue to decrease at a faster rate than these AOGCMs indicate.

The analysis of Arctic ice-cover found significant declines in SIE for 2030, 2060, and 2090 (Fig. 3.2). By 2030, these models projected 90 percent or greater ice coverage in winter, with September cover decreasing to 60 percent. The 2060 model projections decreased to 85 percent winter cover and less than 40 percent September cover.

Table 3.3 displays our results for accessibility in the Arctic Ocean. As a reminder, ice-free means up to 15 percent ice cover in the observed record, and will therefore likely require an ice-strengthened vessel such as a PC-7 Under these scenarios, all routes become accessible for longer periods over the course of the century, changing by as much as two months on each end of the season. Of particular interest, all models show the Northwest Passage as inaccessible in 2030, and some models showed it inaccessible in 2060. However, in 2007, the Northwest Passage was fully navigable for a short period of time. While this demonstrates the enormous variability in conditions, it also illustrates the need for developing models that can accurately simulate rapidly changing Arctic conditions.

3.5 Conclusions and Discussion

Arctic SIE has been decreasing for the past 30 years, and if current trends persist the Arctic Ocean is likely to see an increase in Arctic marine use and coastal development (AMSA 2009). Our analysis of shipping route access to the Arctic based on model projections in 2030, 2060, and 2090 suggests all shipping routes will likely realize expansion of their navigation seasons through the end of the century.

Accuracy of our analysis hinges on whether or not the years 2007-2010 indicate future trends. These years each had less SIE in September than any year before 2007, which may indicate a more rapid decline than the modeled trend. Further, the model

output used a much more conservative emissions scenario than the current global trend, which means these projections are likely to overestimate future SIE (IPCC, 2007; UNMDG, 2010). Therefore, if 2007-2010 turn out to have been precursors rather than anomalies, the models will under-estimate future declines of SIE in the Arctic (Stroeve et al., 2011).

The implications for increased access to the Arctic include greater shipping presence for a longer period of the year. Large variability in sea ice presence from year to year and between regions reduces the predictability of shipping seasons and increases the need for accurate forecasts. Industrial activity in the Arctic is going to be shaped by the periods of access; for example, large scale extraction industries plan several years in advance of operations and need more accurate model projections (AMSA, 2009). Variability and extreme SIE events notwithstanding, continued development of accurate models of sea ice changes can influence the planning and feasibility of economic development in the Arctic.

With increased presence of commercial and industrial ships comes greater risk to the Arctic habitat and significant impacts for Arctic residents. While SIE may decrease dramatically in the coming century, drifting ice will still reach areas that were, for the purposes of this paper, considered ice-free. Therefore, danger will continue to exist both for ice-strengthened vessels and any that do not reach PC-7 standards but may venture north.

In the event of a sinking ship, at least in the immediate future, response times will be much slower in the Arctic than elsewhere because infrastructure is sparse. This creates risk for increased spread of oil and other contaminants before response vessels can be on site. The problem is compounded by the relatively short window of time available in the Arctic before the ocean freezes (AMSA, 2009). Once the freezing seas encapsulate spilled oil, extraction becomes more challenging for several reasons, including the difficulty in accessing Arctic waters in winter. The arctic gyre could move spilled oil across the Arctic Ocean by the following summer, resulting in widely disbursed oil and stressing ecosystems across the Arctic. In a sensitive ecosystem already adapting to the

adverse effects of climate change, a marine oil spill could hasten the possible extinction of several species unique to the Arctic (AMSA 2009). Given these challenges, Arctic nations need to prepare infrastructure that can handle increased Arctic marine use. This requires greater planning through the Arctic Council and the International Maritime Organization to prevent harm to Arctic ecosystems and the people who live there.

3.7 Tables

Table 3.1 The Arctic Guidelines and the Unified Requirements, from AMSA (2009). The Polar Code designates "a system of polar classes for ships with different levels of capability and construction, structural and equipment requirements under various ice conditions. The Unified Requirements apply to ships of member associations constructed on or after March 1, 2008" (AMSA, 2009: 56).

Polar Class	General Description
PC-1	Year-round operation in all Arctic ice-covered waters
PC-2	Year-round operation in moderate multi-year ice conditions
PC-3	Year-round operation in second-year ice which may include multi-year ice inclusions
PC-4	Year-round operation in thick first-year ice which may include old ice inclusions
PC-5	Year-round operation in medium first-year ice which may include old ice inclusions
PC-6	Summer/autumn operation in medium first-year ice which may include old ice inclusions
PC-7	Summer/autumn operation in thin first-year ice which may include old inclusions.

Table 3.2 Observed trends and simulated SIE. SIE in million square kilometers of sea ice. The observed 2000-2008 is the mean sea SIE for nine years. The model mean represents the mean SIE computed for the four models. Trend 1 is the trend of observed SIE from 1980-2008. Trend 2 is the trend of SIE from 1980-2006.

	March, km^2	September, km^2
Observed 2000-2008	14.7	5.4
2030 Model Mean	14.9	4.6
2060 Model Mean	13.7	2.2
2090 Model Mean	12.8	0.4
Extended Trend 1 - 2030	13.5	3.3
Extended Trend 1 - 2060	12.1	0.9
Extended Trend 1 - 2090	10.7	0
Extended Trend 2 - 2030	13.6	4
Extended Trend 2 - 2060	12.2	2.1
Extended Trend 2 - 2090	10.9	0.2

Table 3.3 Arctic marine access. For the observed record and simulations, ice-free conditions are based on less than 15 percent ice cover. The top section is the first month that each route was or will be accessible for the given years; the bottom section is the first month of inaccessibility. A range of months indicates that the models showed a range of possibilities.

First Month Accessible	**2000-2008 Observed**	**AOGCM Simulated Accessibility**		
		2030	**2060**	**2090**
Bering Strait	June	June	June	May-June
Northeast Passage	Inaccessible	August-September or Inaccessible	August-September	July-August
Northwest Passage	Inaccessible	Inaccessible	August-September or Inaccessible	August
Arctic Bridge	July	July	June-July	June-July
First Month Inaccessible	**2000-2008 Observed**	**2030**	**2060**	**2090**
Bering Strait	December	December	December-January	January-February
Northeast Passage	Inaccessible	October	October-November	October-December
Northwest Passage	Inaccessible	Inaccessible	October	October-November
Arctic Bridge	November	November-December	December	December-January

3.6 Figures

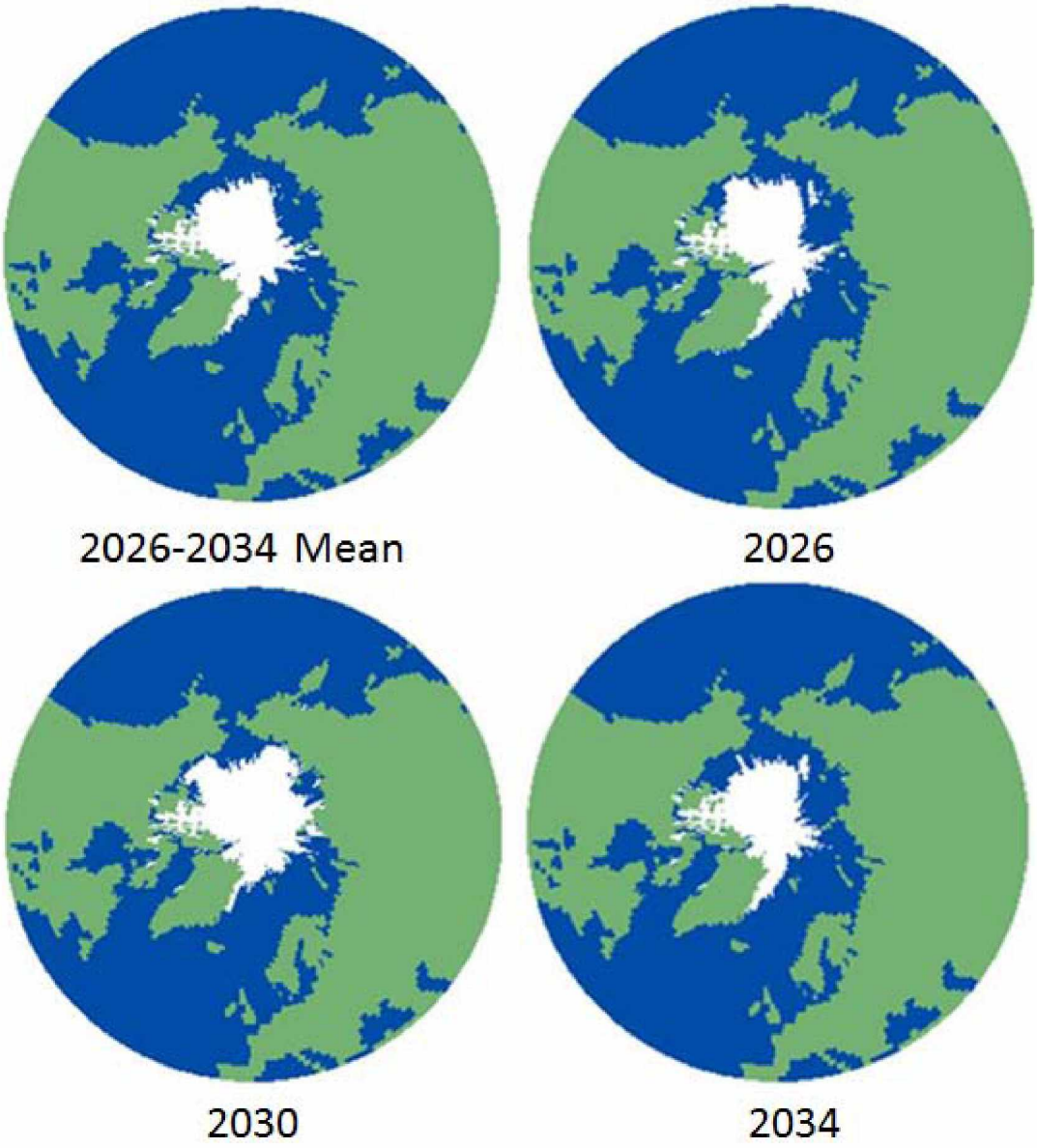

Figure 3.1 Year to year projection variability, 2026-2034. Example of variability in year to year SIE Output for September. HadGem's nine-year mean, 2026, 2030, and 2034.

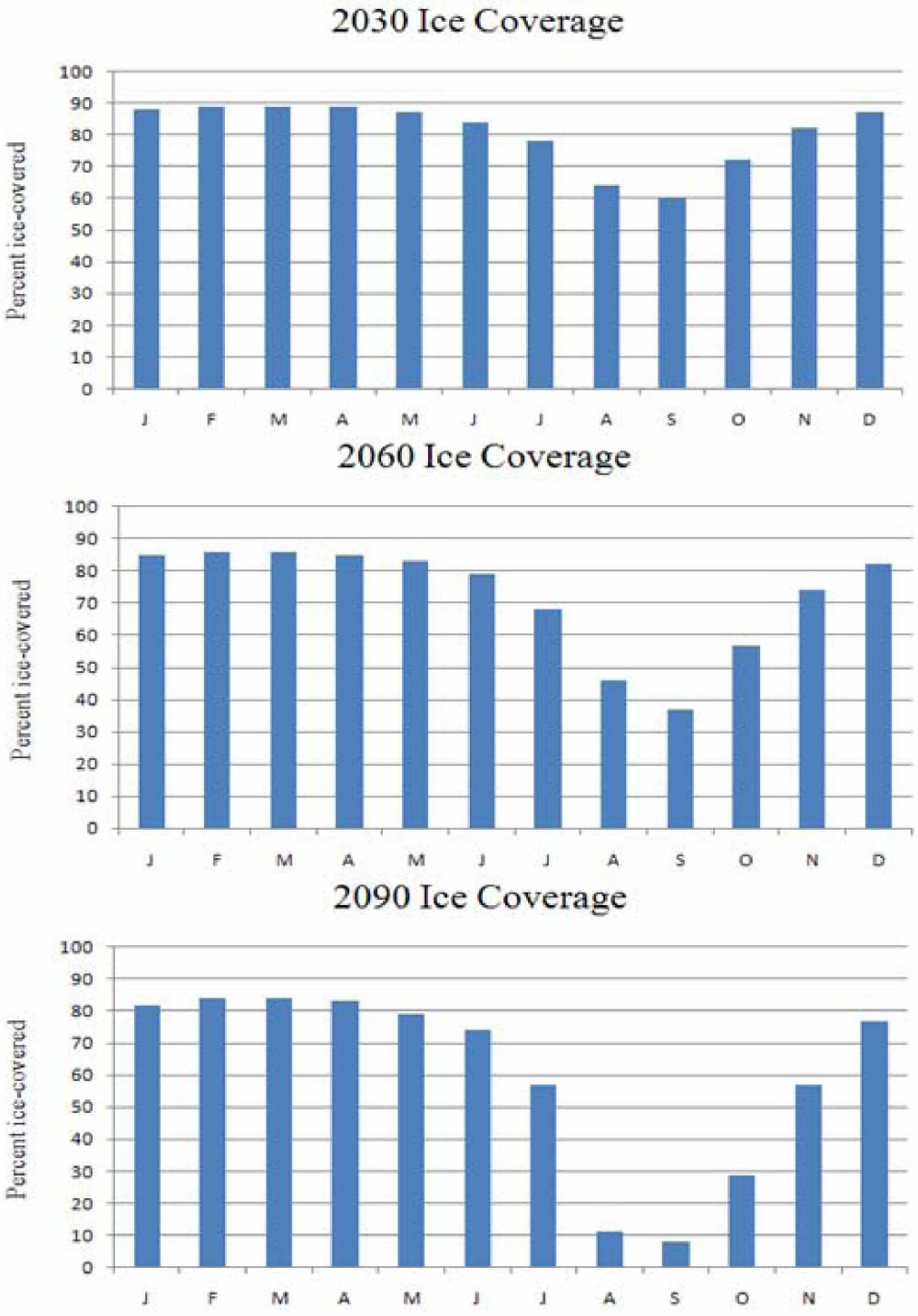

Figure 3.2 Arctic sea ice coverage, 2030, 2060, and 2090. Ice coverage by percent from January through December, averaged over four models.

3.8 References

ACIA, 2005. Arctic Climate Impact Assessment. Cambridge University Press. 1024p. http://www.acia.uaf.edu. Accessed July 26, 2011.

AMSA. 2009. Arctic Marine Shipping Assessment 2009 Report. Arctic Council, April 2009. http://www.pame.is/amsa. Accessed July 26, 2011.

Arzel, O., Fichefet, T., and Goosse, H. 2006. Sea ice evolution over the 20th and 21st centuries as simulated by current AOGCMs. Ocean Modelling 12 (2006) 401-415.

Boé, J., Hall., A., and Qu, X. 2009. September sea-ice cover in the Arctic Ocean projected to vanish by 2100. Nature Geoscience. doi: 10.1038/NGEO467.

Brigham, L. 2007. Thinking about the Arctic's future: scenarios for 2040. The Futurist. Vol. 41(5). 27-34.

Brigham, L. 2010. The fast-changing maritime Arctic. *U.S. Naval Institute Proceedings* 136.

IPCC. 2007. Climate change 2007: the physical science basis—contribution of Working Group I to the Fourth Assessment Report. Cambridge: Cambridge University Press.

Shein, K.A., ed. 2006. State of the climate in 2005. Bullet of the American Meteorological Society, 87, S1-102.

Stroeve, J., Holland, M., Meier, W., Scambos, T., and Serreze, M. 2007. Arctic sea ice decline: Faster than forecast. Geophysical Research Letters 34, L095101, doi: 10.1029/2007GL029703.

Stroeve, J., Serreze, M., Holland, M., Kay, J., Malanik, J., and Barret, A. 2011. The Arctic's rapidly shrinking sea ice cover: a research synthesis. Climatic Change. doi: 10.1007/s10584-011-0101-1.

UNMDG. 2010. United Nations Statistics Division, Millennium Development Goals indicators: Carbon dioxide emissions (CO2). http://mdgs.un.org/unsd/mdg/SeriesDetail.aspx?srid=749&crid=. Accessed July 26, 2011.

Wang, M. and Overland, J. 2009. A sea ice free summer Arctic within 30 years? Geophysical Research Letters. Vol. 36, L07502, doi: 10.1029/2009GL037820

Winton, M. 2011. Do climate models underestimate the sensitivity of Northern Hemisphere sea ice cover? Journal of Climate. doi: 10.1175/2011JCLI4146.1

Zhang, X. 2010. Sensitivity of Arctic summer sea ice coverage to global warming forcing: towards reducing uncertainty in Arctic climate change projections. Tellus: Series A. Vol. 62 (3). 220-227.

Zhang, X., and Walsh, J. 2006. Toward a seasonally ice-covered Arctic Ocean: scenarios from the IPCC AR4 model simulations. Journal of Climate 19. 1730-1747.

Appendix 3.1

This appendix includes model output for the Bering Strait, Northeast Passage, Northwest Passage, and the Arctic Bridge. For each route, model output is given for 2030, 2060, and 2090. However, not all months are shown in the appendix. The images included represent the first month that each route is open and the first month that each route is closed. When models displayed the same results for opening or closing month, only one image from those models was shown to prevent redundancy. As there are four models and four routes investigated, each model took preference for one of the routes, to ensure the models are equally represented in the appendix. See captions for indicated year and month of projection.

Bering Strait

CCSM June 2030

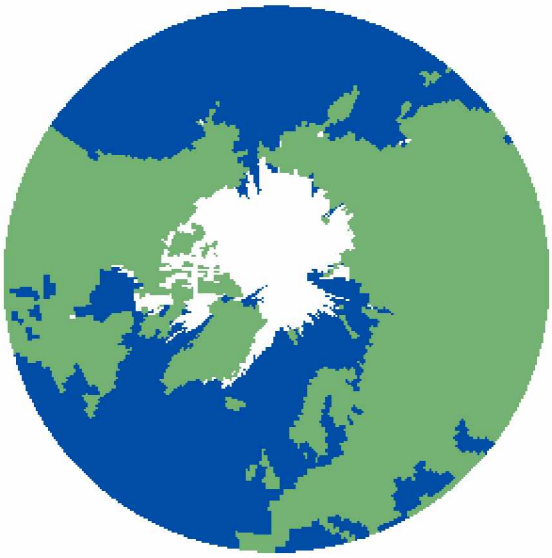

CCSM December 2030

CCSM June 2060

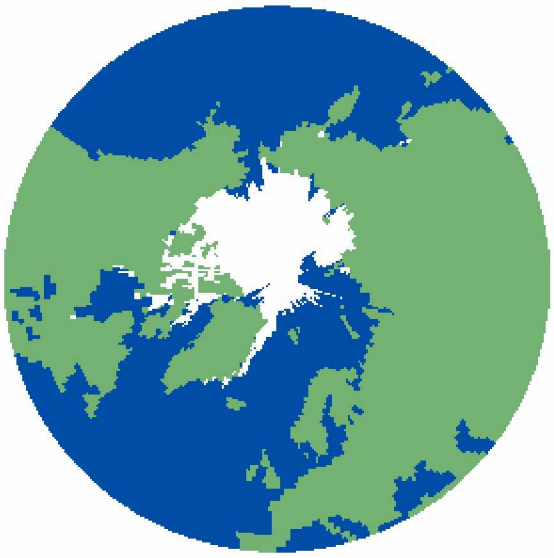

CCSM December 2060

HadGEM January 2060

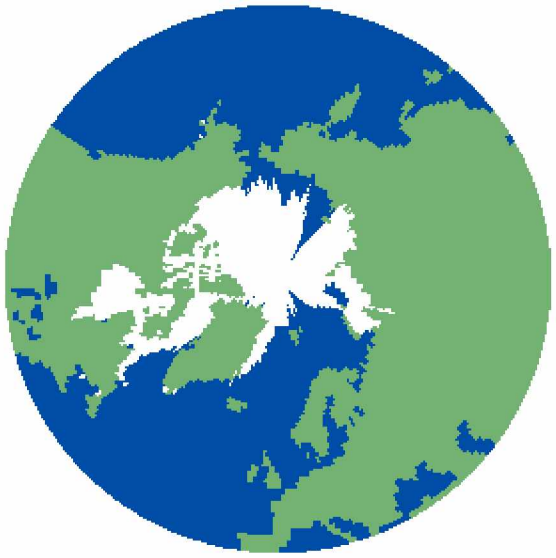

HadGEM May 2090

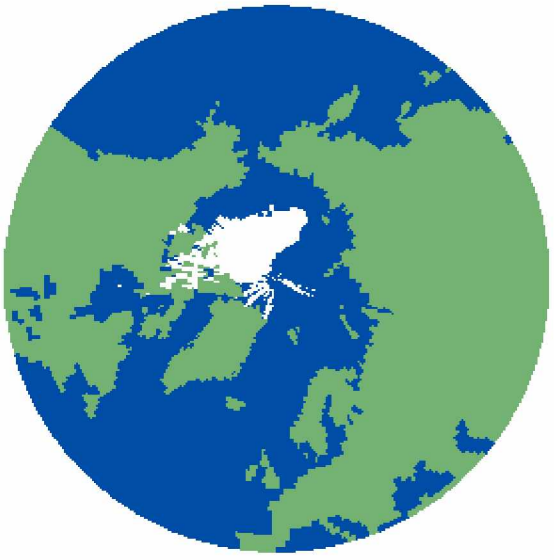

CCSM June 2090

HadGEM January 2090

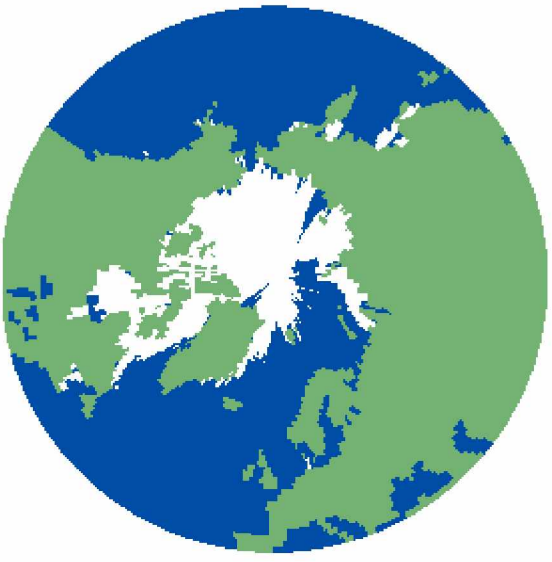

CCSM February 2090

Northeast Passage

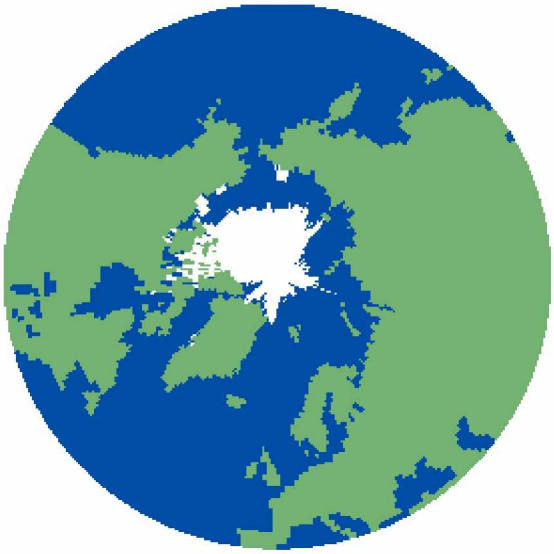

CCSM August 2030

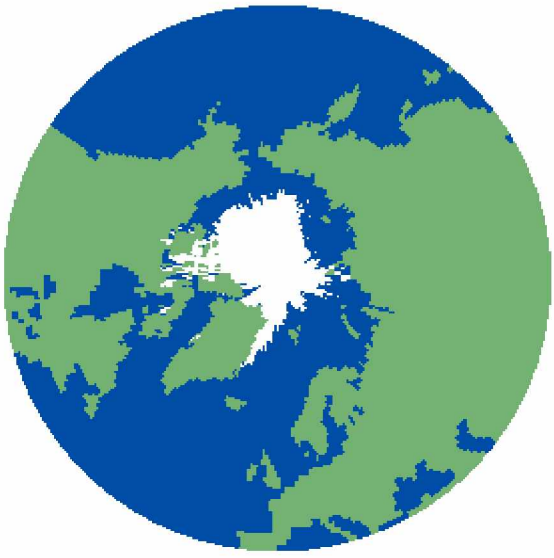

HadGEM September 2030

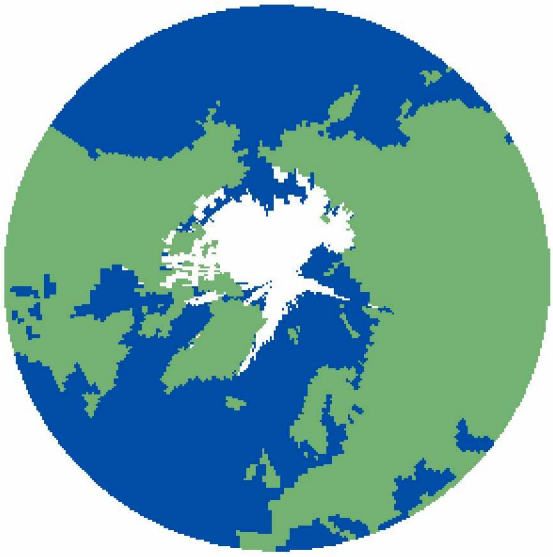

CCSM October 2030

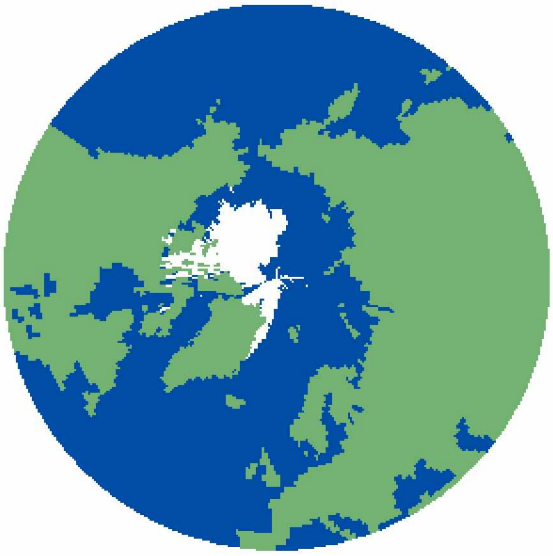

HadGEM August 2060

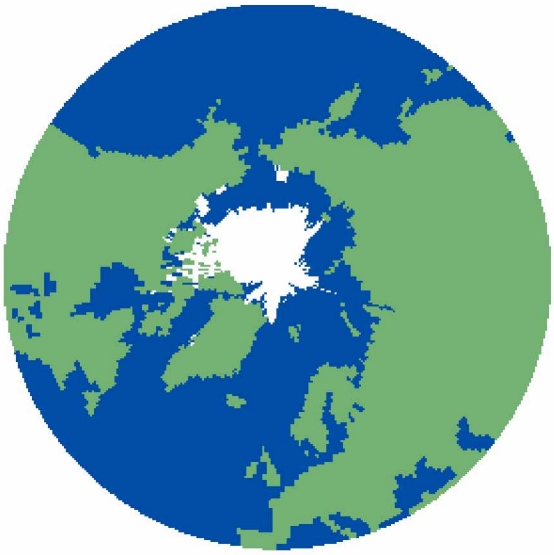

MRCM September 2060

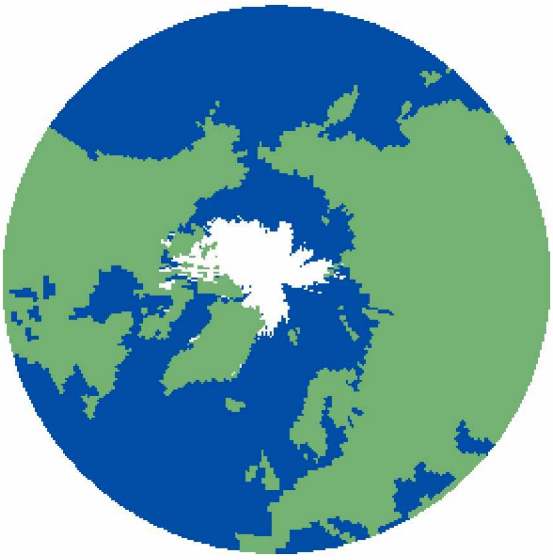

IPSL October 2060

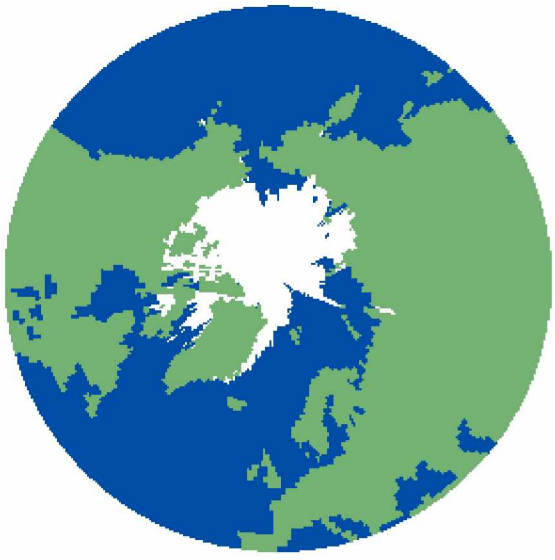

HadGEM November 2060

HadGEM July 2090

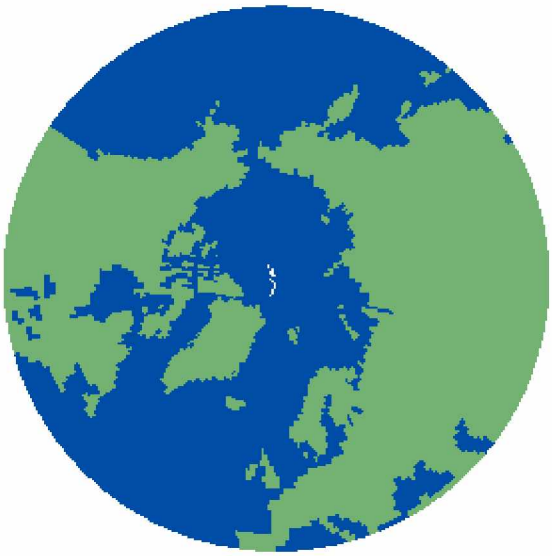

MRCM August 2090

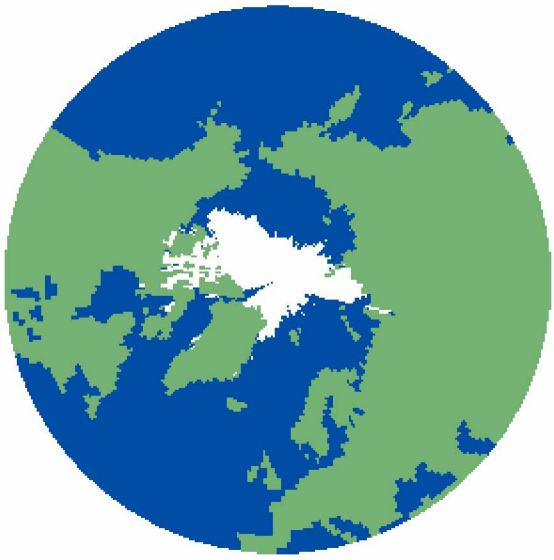

IPSL October 2090

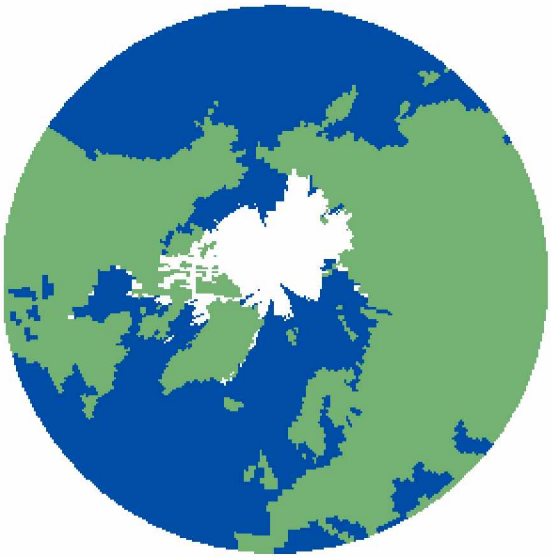

MRCM November 2090

HadGEM December 2090

Northwest Passage

IPSL September 2030

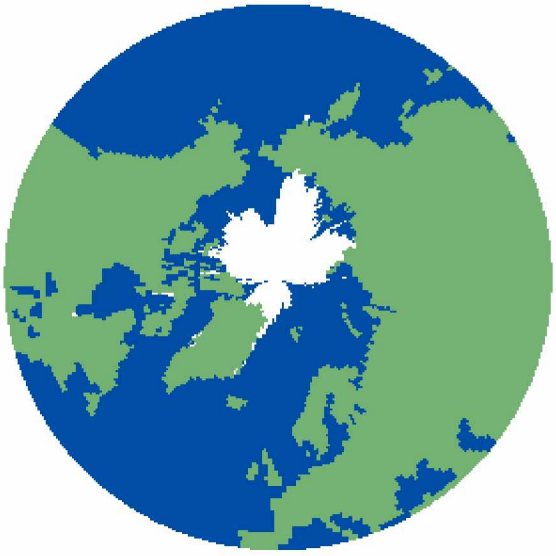

MRCM August 2060

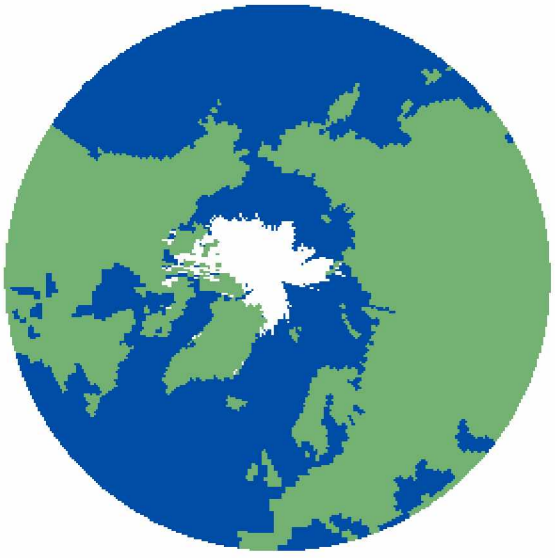

IPSL September 2060

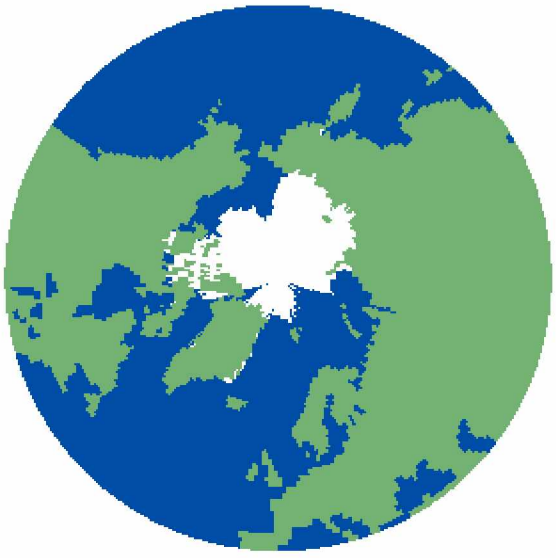

MRCM October 2060

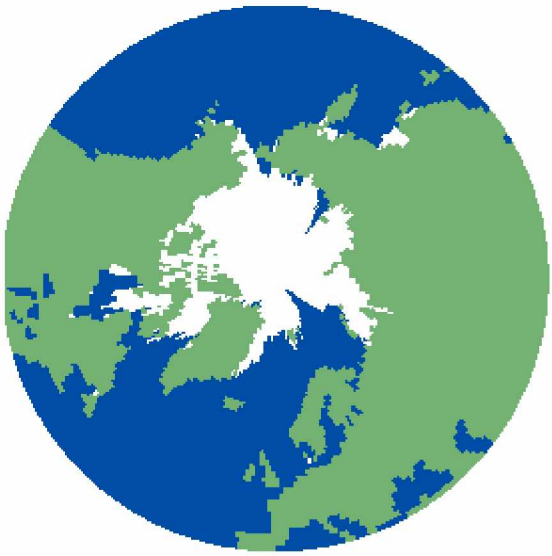

MRCM November 2060

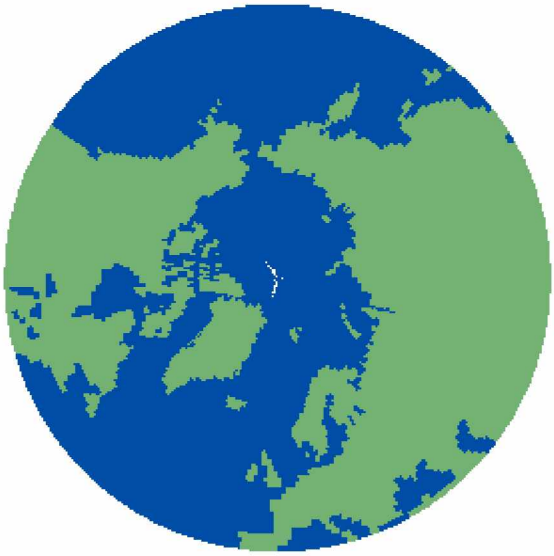

MRCM August 2090

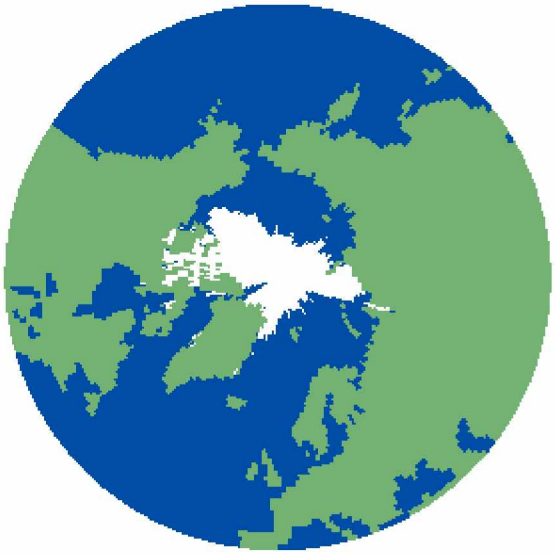

IPSL October 2090

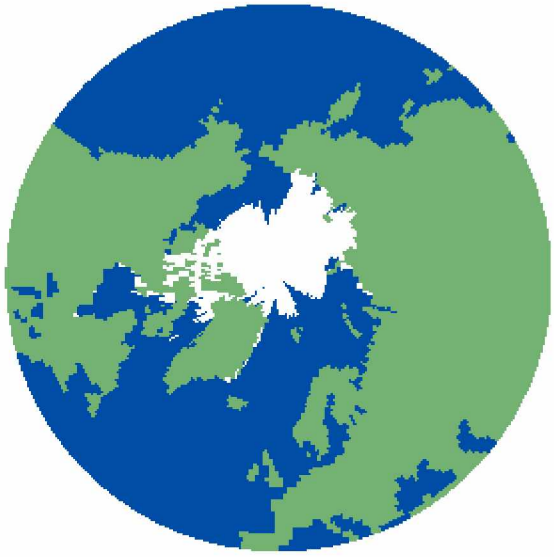

MRCM December 2090

Arctic Bridge

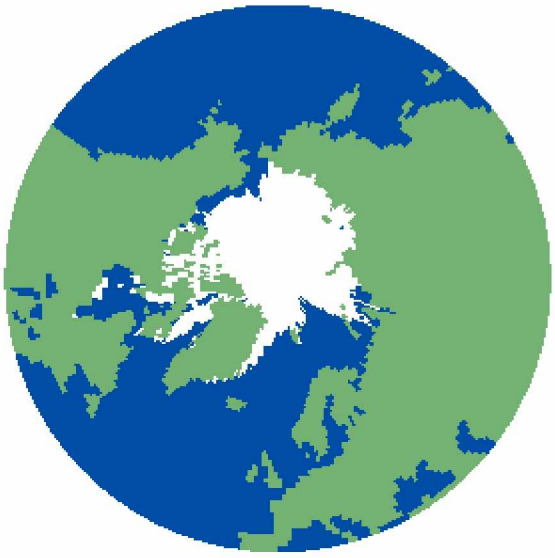

MRCM July 2030

IPSL November 2030

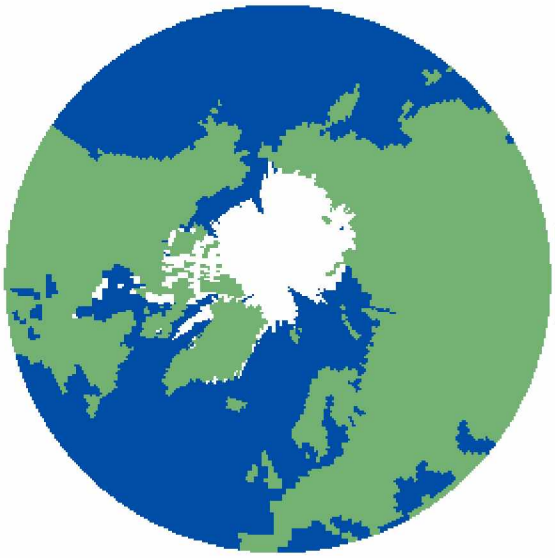

MRCM June 2060

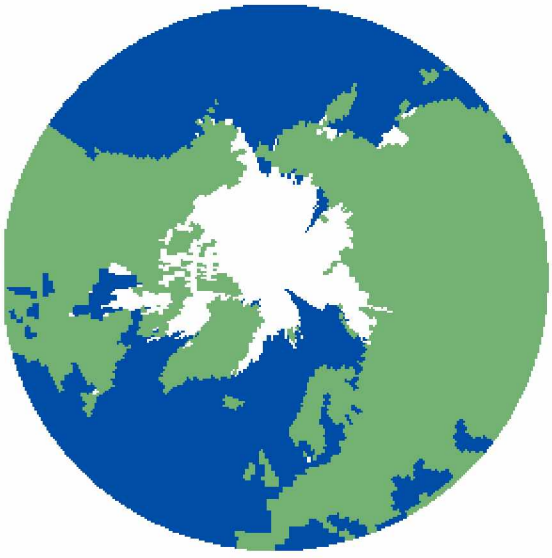

MRCM November 2060

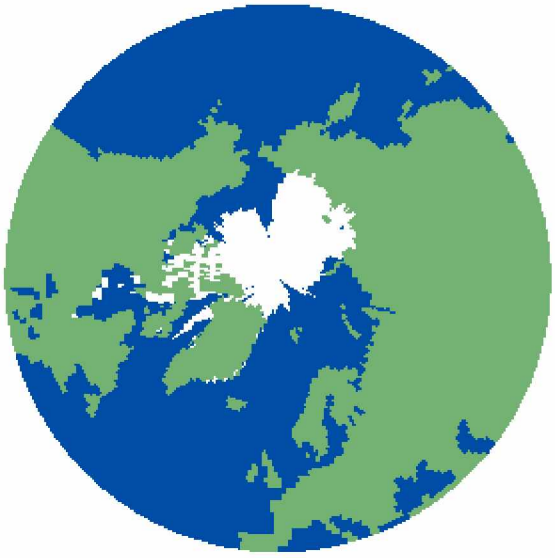

MRCM June 2090

HadGEM July 2090

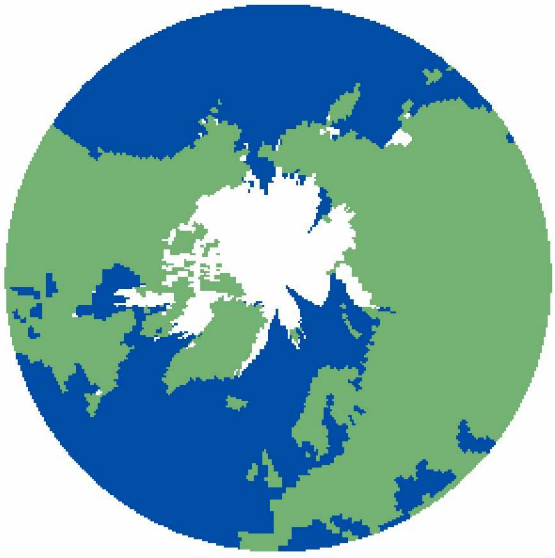

MRCM December 2090

HadGEM January 2090

Conclusion

The objective of Chapter 1 was to investigate regional variations and drivers in sea ice, using the longitudinal divisions of the ACIA (2005). Our study found significant variability among regions, particularly in the Atlantic quadrant.

We tested a two-part hypothesis: warming Atlantic Ocean sea surface temperatures (SSTs) result in decreased winter sea ice extent (SIE) in the Atlantic quadrant; and Arctic winds increase summer SIE in the Atlantic quadrant. Our analysis revealed SSTs to be statistically significant for September SIE in all quadrants of the Arctic and also for March SIE trends in both the Atlantic and Russian quadrants. However, contrary to our hypothesis, it appears that changes in SIE in the Atlantic region may result in warmer SSTs. Wind magnitude associations do not appear to increase the quantity of sea ice in the Atlantic quadrant – the statistically significant relationships between SIE and Arctic winds were in the Pacific quadrant and pan-Arctic SIE only. Finally, the combined influence of Arctic wind magnitudes and SSTs were not important for the Atlantic quadrant, but much greater significance for the Pacific quadrant.

Chapter 2 investigated atmosphere ocean general circulation model (AOGCM) performance in the Arctic and ACIA defined regional quadrants and identified the models that were most successful in retrospective simulations of SIE from 1980-2008. Because sea ice loss varies by region, the most useful models will be constructed in ways that capture regional differences; in addition to other variables, model performance depended on the evaluation region. SIE analysis by ACIA quadrants identified that the trends as well as model performance vary by region.

Sea ice models that included more sophisticated sea ice physics appeared to perform more accurately than other models. While model resolution may not have a significant effect on model output, some sea ice characteristics will require finer spatial resolution, such as coastal interactions, and ice salinity and thickness. Similar to other evaluative studies (Arzel et al., 2006; Zhang and Walsh, 2006; Stroeve et al., 2007; Wang and Overland, 2009; Zhang, 2010), this research indicates that SIE changes are occurring faster than almost any model projections, particularly for the period 2000-2008. Overland

and Wang (2007) is the only previous study to investigate model performance by region based on Arctic seas. Our work is the first to utilize the ACIA division for the purpose of evaluating AOGCM performance of SIE. Further, it provides the first synthesis of AOGCM evaluations from the peer-reviewed literature.

We identified four models that best simulated the observed trends, both on regional and pan-Arctic scales. Selecting models that best simulate sea ice dynamics regionally can provide new tools for policy-makers, arctic planners, and residents within those regions as they address climate change impacts and opportunities.

In Chapter 3, we determined that Arctic SIE will continue to decrease at a rapid rate over the next century, particularly in August and September. We applied simulated sea ice conditions of the best performing models (Chapter 2) to explore scenarios of marine access and resource development in the Arctic. We found that all Arctic shipping routes will become significantly more accessible in 2030, 2060, and 2090, but with variability between models and regions. Increased access may lead to new economic opportunities for Arctic nations, shipping industries, and resource developers. These changes also increase the likelihood of Arctic marine disasters in regions that, while increasingly accessible, remain distant from the kinds of infrastructure commonly found along major trade routes. While some studies have used model projections to investigate Arctic accessibility (AMSA, 2009), this study is the first to analyze Arctic accessibility with a suite of AOGCMs that are ranked by performance (relative to observed trends) and region.

ACIA identified geographic regions to examine the human dimensions of climate change: studying sea ice changes within these regions provides new insights for understanding physical, social, and economic impacts. Climate change and the magnitude of the associated impacts are expected to vary across the Arctic. While pan-Arctic studies are necessary for understanding the broader system of climate change, regional studies translate directly to the needs of people across the Arctic, especially since trends and drivers vary regionally.

Each chapter of this study added new findings to the scientific body of literature regarding Arctic sea ice dynamics. Chapter 1 identified that changing SIE may be altering Atlantic Ocean SSTs. Chapter 2 identified the best performing models in the Arctic and by region. In addition, we synthesized the results of several studies of model performance in the Arctic. Chapter 3 analyzed a range of sea ice scenarios to determine potential future impacts and opportunities on Arctic shipping and resource development.

The continued decline of Arctic sea ice coverage will vary by region, but is expected to result in a myriad of challenges for coastal regions, Indigenous populations, and endangered and threatened species across the Arctic. Simultaneously, dramatic shifts in sea ice regimes bring new opportunities for Arctic marine trade routes and resource development. AOGCMs must continue to improve in sophistication and accuracy to provide more in-depth interpretation of future scenarios; Arctic nations and regional industries need these improved forecasts to prepare for the impacts and opportunities posed by climate change.

References

ACIA, 2005. Arctic Climate Impact Assessment. Cambridge University Press. 1024p. http://www.acia.uaf.edu Accessed July 26, 2011.

AMSA. 2009. Arctic Marine Shipping Assessment 2009 Report. Arctic Council, April 2009. http://www.pame.is/amsa. Accessed July 26, 2011.

Arzel, O., Fichefet, T., and Goosse, H. 2006. Sea ice evolution over the 20th and 21st centuries as simulated by current AOGCMs. Ocean Modelling 12 (2006) 401-415.

Boé, J., Hall., A., and Qu, X. 2009. September sea-ice cover in the Arctic Ocean projected to vanish by 2100. Nature Geoscience. doi: 10.1038/NGEO467.

Cavalieri, D., Parkinson, C., Gloersen, P., and Zwally, H.J. 1996, updated 2008. Sea ice concentrations from Nimbus-7 SMMR and DMSP SSM/I passive microwave data, [1980-2007]. Boulder, CO USA: National Snow and Ice Data Center. Digital Media.

Comiso, J., Parkinson, C., Gersten, R., and Stock, L. 2008. Accelerated decline in the Arctic sea ice cover. Geophysical Research Letters 35, L01703, doi: 10.1029/2007GL031972.

Fetterer, F., Knowles, K., Meier, W., and Savoie, M. 2009. Sea Ice Index. Boulder, Colorado USA: National Snow and Ice Data Center. Digital Media.

IPCC. 2007. Climate change 2007: the physical science basis—contribution of Working Group I to the Fourth Assessment Report. Cambridge: Cambridge University Press.

Maslowski, W, Kinney, J.C., Jakacki, J., and Zwally, J. 2008. State of the Arctic sea ice. Geophysical Research Abstracts. Vol. 10.

Meier, W., Fetterer, F., Knowles, K., Meier, W., Savoie, M., and Brodzik, M.J. 2006, updated quarterly. Sea ice concentrations from Nimbus-7 SMMR and DMSP SSM/I passive microwave data [2008]. Boulder, CO USA: National Snow and Ice Data Center. Digital media.

NSIDC. 2010. Arctic sea ice falls to third-lowest extent. National Snow and Ice Data Center, 10-4-2010. http://www.nsidc.org/news/press/20101004_minimumpr.html. Accessed July 26, 2011.

Overland, J.E., and Wang, M. 2007. Future regional Arctic sea ice declines. Geophysical Research Letters 34. doi: 10.1029/2007GL030808.

Parkinson, C., and Cavalieri, D. 2008. Arctic sea ice variability and trends, 1979-2006. Journal of Geophysical Research, 113, C07003, doi: 10.1029/2007JC004558.

Perovich, D., Meier, W., Maslanik, J., and Richter-Menge, J. Sea Ice Cover [in Arctic Report Card 2010]. http://www.arctic.noaa.gov/reportcard.

Polyak, L., Alley, R., Andrews, J., Brigham-Greet, J., Cronin, T., Darby, D., Dyke, A., et al. 2010. History of sea ice in the Arctic. Quarternary Science Reviews; doi: 10.1016/j.quascirev.2010.02.010.

Richter-Menge, J., and Overland, J.E., Eds. 2010: Arctic Report Card 2010. http://www.arctic.noaa.gov/reportcard. Accessed July 26, 2011.

Stroeve, J., Holland, M., Meier, W., Scambos, T., and Serreze, M. 2007. Arctic sea ice decline: Faster than forecast. Geophysical Research Letters 34, L095101, doi: 10.1029/2007GL029703.

Stroeve, J., Serreze, M., Holland, M., Kay, J., Malanik, J., and Barret, A. 2011. The Arctic's rapidly shrinking sea ice cover: a research synthesis. Climatic Change. doi: 10.1007/s10584-011-0101-1.

Wang, M. and Overland, J.E. 2009. A sea ice free summer Arctic within 30 years? Geophysical Research Letters. Vol. 36, L07502, doi: 10.1029/2009GL037820

Zhang, X. 2010. Sensitivity of Arctic summer sea ice coverage to global warming forcing: towards reducing uncertainty in Arctic climate change projections. Tellus: Series A. Vol. 62 (3). 220-227.

Zhang, X., and Walsh, J. 2006. Toward a seasonally ice-covered Arctic Ocean: scenarios from the IPCC AR4 model simulations. Journal of Climate 19. 1730-1747.